Western Graduate&PostdoctoralStudies

Western University

Scholarship@Western

Electronic Thesis and Dissertation Repository

8-20-2013 12:00 AM

Elucidating the role of cathepsin B in the lifecycle of influenza A virus

Macon D. Coleman
The University of Western Ontario

Supervisor
Dr. Sung Kim
The University of Western Ontario

Graduate Program in Microbiology and Immunology
A thesis submitted in partial fulfillment of the requirements for the degree in Master of Science
© Macon D. Coleman 2013

Follow this and additional works at: https://ir.lib.uwo.ca/etd

Part of the Immunology and Infectious Disease Commons

Recommended Citation

Coleman, Macon D., "Elucidating the role of cathepsin B in the lifecycle of influenza A virus" (2013). *Electronic Thesis and Dissertation Repository*. 1551.
https://ir.lib.uwo.ca/etd/1551

This Dissertation/Thesis is brought to you for free and open access by Scholarship@Western. It has been accepted for inclusion in Electronic Thesis and Dissertation Repository by an authorized administrator of Scholarship@Western. For more information, please contact wlswadmin@uwo.ca.

ELUCIDATING THE ROLE OF CATHEPSIN B IN THE LIFECYCLE OF INFLUENZA A VIRUS

Thesis format: Monograph

by

Macon Coleman

Graduate Program in Microbiology & Immunology

A thesis submitted in partial fulfillment
of the requirements for the degree of
Master of Science

The School of Graduate and Postdoctoral Studies
The University of Western Ontario
London, Ontario, Canada

© Macon Coleman, 2013

Abstract

Influenza virus type A (IVA) is the etiologic agent responsible for the febrile respiratory illness referred to as the flu. Seasonal and occasionally pandemic IVA-associated illness is a significant cause of morbidity and mortality worldwide, and presents a significant burden to the healthcare system. Our previous work showed that the propagation of IVA required the lysosomal protease cathepsin B (CTSB), though the mechanism behind this dependency was not elucidated. This study further assessed the role of CTSB by examining different stages in the viral lifecycle for defects using CTSB-deficient (CTSB$^{-/-}$) macrophages and the CTSB-specific chemical inhibitor CA-074 Me (CaMe) in human lung epithelial cells. CTSB$^{-/-}$ and CA-074 Me-treated cells showed no defect in either the uptake of virus particles, nor their replication following endosomal escape compared to wildtype or non-treated cells, respectively. However, CTSB$^{-/-}$ and CA-074 Me-treated cells had significantly less hemagglutinin (HA) protein both inside and on the surface of infected cells, as determined by both Western blotting and confocal immunofluorescence microscopy. These results suggest that CTSB is required for a step(s) in the viral lifecycle following entry into host cells, either before or during the synthesis of viral proteins, and possibly during the transport of viral components to the host membrane. Further work is necessary to determine the mechanistic details of these observations, and may yield novel potential therapies for influenza infections.

Keywords

Cathepsin B, Influenza A virus, CA-074 Me, Hemagglutinin

Acknowledgements

I would like to thank Dr. Sung Kim, as well as present and past members of the Kim lab for their guidance, assistance, and impartment of both technical expertise and their wealth of knowledge. I also wish to thank members of the McCormick lab for their help throughout the duration of this project.

I would like to acknowledge Dr. Mansour Haeryfar for generously providing the virus used for these studies, and both Delfina Mazzuca and Jin Hayatsu for their assistance with the virus.

I would like to thank my advisory committee members Dr. Mansour Haeryfar, Dr. Gregory Dekaban and Dr. Stephen Barr for constructive feedback and suggestions which were instrumental in the development and execution of this research.

I also wish to thank Dr. Katherine Kasper for her mentorship and support during my time as a graduate student. Her friendship has been invaluable in my success both as a student and a scientist.

Finally, I would like to thank my family and friends for their continued support; your love and encouragement has made this work possible. Words cannot express my gratitude for all that you bring into my life.

Table of Contents

Abstract ii

Acknowledgements iii

Table of Figures vi

Table of Appendices vii

Abbreviations viii

Chapter 1: Introduction 1

- 1.1 Influenza A Virus 1
  - 1.1.1 IVA Structure 1
  - 1.1.2 IVA Genetics 4
  - 1.1.3 IVA Lifecycle 5
  - 1.1.4 Hemagglutinin 9
- 1.2 Cathepsin B 10
  - 1.2.1 Background 10
  - 1.2.2 The role of Cathepsin B in viral lifecycles 11
  - 1.2.3 Potential involvement of Cathepsin B in lipid homeostasis 12
- 1.3 Rationale, hypothesis and objectives 13

Chapter 2: Methods 14

- 2.1 Reagents 14
- 2.2 Cell Culture 14
- 2.3 Viral Infections 15
- 2.4 Western Blot 15
- 2.5 RT-qPCR 15
- 2.6 Fractionation 16
- 2.7 Cholesterol Assay 17
- 2.8 Protein Assay 17
- 2.9 Immunofluorescence Microscopy 17
- 2.10 Hemagglutination Assay 18
- 2.11 MTT Assay 18
- 2.12 Statistical Analysis 19

Chapter 3: Results 20

3.1 The role of CTSB in influenza A virus entry and replication 20

3.1.1 CTSB is not required for influenza virus entry and replication in BMDIM cells ..23

3.1.2 CTSB is not required for influenza virus entry and replication in A549 cells 23

3.2 The role of CTSB in viral HA protein production 23

3.2.1 A deficiency in CTSB reduces viral HA protein production in BMDIM cells 30

3.2.2 A deficiency in CTSB reduces viral HA protein production in A549 cells 30

3.3 Pharmacological inhibition of CTSB reduces surface expression of HA protein on infected cells 30

3.4 Pharmacological inhibition of CTSB reduces intracellular HA protein in infected cells 44

3.5 Cholesterol does not accumulate in a CTSB-dependent manner 44

Chapter 4: Discussion 50

4.1 CTSB is not required for influenza A virus entry or replication 50

4.2 A deficiency in CTSB reduces viral HA protein production 52

4.3 Pharmacological inhibition of CTSB reduces surface expression of HA protein on infected cells 53

4.4 Pharmacological inhibition of CTSB reduces intracellular HA protein in infected cells 56

4.5 Cholesterol does not accumulate in a CTSB-dependent manner 58

4.6 Future directions 60

Chapter 5: References 63

Chapter 6: Appendices 77

Chapter 7: Curriculum Vitae 85

Table of Figures

Figure 1 – Structure of influenza virus 2

Figure 2 – Overview of the IVA lifecycle 6

Figure 3 – Standard curves of qPCR Ct values for known concentrations of amplicon. 21

Figure 4 – Viral entry and replication are not significantly different between wildtype and $CTSB^{-/-}$ cells. 24

Figure 5 – Toxicity of ActD in C57 and A549 cells. 26

Figure 6 – Viral entry and replication are not significantly different in CaMe-treated A549 cells. 28

Figure 7 – $CTSB^{-/-}$ cells produce significantly less viral HA protein. 31

Figure 8 – Primary $CTSB^{-/-}$ cells produce less viral HA protein compared with Wt. 33

Figure 9 – A549 cells treated with 150 μM CaMe produce significantly less viral HA protein. 35

Figure 10 – Vehicle control for CaMe treatment of A549 cells. 37

Figure 11 – Toxicity of CaMe in A549 cells. 39

Figure 12 – Inhibition of CTSB in A549 cells with 150 μM CaMe reduces surface expression of HA protein. 41

Figure 13 – Inhibition of CTSB in A549 cells with 150 μM CaMe reduces intracellular expression of HA protein. 45

Figure 14 – Endosomal cholesterol accumulation is not responsible for CTSB-dependent influenza A virus restriction 48

Table of Appendices

Appendix 1 – ActD blocks the production of viral HA protein at a concentration of 5 µg/mL. 77
Appendix 2 – Detected copy numbers of HA and MA per titred virion in the inoculum. 79
Appendix 3 – Immunofluorescence microscopy of infected A549 cells stained with 2□ antibody (FITC) only. 81
Appendix 4 – Hemagglutination assay of infected A549 supernatants 83

Abbreviations

ActD	Actinomycin D
BMDIM	Bone marrow derived immortalized macrophages
BSA	Bovine serum albumin
CaMe	CA-074 Me; L-3-*trans*-(Propylcarbamyl)oxirane-2-carbonyl)-L-isoleucyl-L-proline methyl ester
CTSB	Cathepsin B
DMSO	Dimethyl sulfoxide
FBS	Fetal bovine serum
FITC	Fluorescein isothiocyanate
HA	Hemagglutinin
HIV	Human immunodeficiency virus
HSV-1	Herpes simplex virus 1
IB	Immunoblot
IVA	Influenza virus type A
kDa	Kilodalton
MA	Matrix protein
MDCK	Madin-Darby canine kidney cells
µg	Microgram
µL	Microliter
µm	Micrometer
µM	Micromolar
MOI	Multiplicity of infection
MTT	3-(4,5-Dimethylthiazol-2-yl)-2,5-diphenyltetrazolium bromide
NA	Neuraminidase
nm	Nanometer
PR8	Influenza A H1N1/Puerto Rico/8/34
RNA	Ribonucleic acid
RT-qPCR	Reverse transcriptase quantitative polymerase chain reaction
SDS PAGE	Sodium dodecyl sulfate polyacrylamide gel electrophoresis

Chapter 1: Introduction

1.1 Influenza A Virus

Viruses are obligate infectious particles composed of genetic material surrounded by a protein capsid and in some cases a lipid envelope. Influenza viruses can be divided into three genera within the *Orthomyxoviridae* family, each containing a single species: Influenza virus A, B and C. Infection in humans results in a febrile disease characterized by malaise, cough and headache, commonly referred to as the "flu" [1]. While illness resulting from influenza virus infection is usually self-limiting – resolving within a week – some isolates are capable of causing severe illness and even death [2]. Complications resulting from infections can be equally serious, and include pneumonia due to secondary bacterial infections, pulmonary and cardiovascular disease [3, 4]. In addition to humans, influenza viruses also infect a number of vertebrates, including birds, pigs, and other mammals. Infections in domestic livestock have occasionally resulted in the transfer of influenza to humans, and subsequent outbreaks of the disease [5]. Infections in migratory birds pose the greatest threat, and raise concerns of a global influenza pandemic.

Although all three species of influenza virus have the capacity to infect humans, infections with influenza virus type A (IVA) are the most common [6, 7]. In the most recent flu season, the Centers for Disease Control (CDC) reported 86% of 22417 laboratory-confirmed influenza infections were due to IVA, and the remaining 14% to type B influenza virus [8] – type C influenza virus was rarely isolated [9]. Due to its prevalence and body of existing research knowledge, IVA was selected for these studies.

1.1.1 IVA Structure

IVA is an enveloped virus with a genome consisting of eight negative-sense single-stranded RNA (-ssRNA) segments (Figure 1). These genome segments code for eleven proteins, eight of which are packaged into progeny virions [10]. Two of these proteins, hemagglutinin (HA), which mediates entry, and neuraminidase (NA), which facilitates progeny virion release from cells [11, 12], are expressed on the surface of virions as spike glycoproteins and are therefore the antigenic determinants against which humoral immune responses are raised.

Figure 1 – Structure of influenza virus

The surface of the enveloped virion is studded with hemagglutinin (HA) and neuraminidase (NA) envelope glycoproteins. Beneath the host-derived lipid envelope, matrix (MA) proteins surround the ribonucleoprotein core, which contains the negative-sense segmented RNA genome of the virus. These eight segments encode viral polymerase subunits (PB2, PB1, PA), hemagglutinin protein (HA), nucleoprotein (NP), neuraminidase (NA), matrix and M2 proteins (M), and non-structural proteins 1 and 2 (NS).

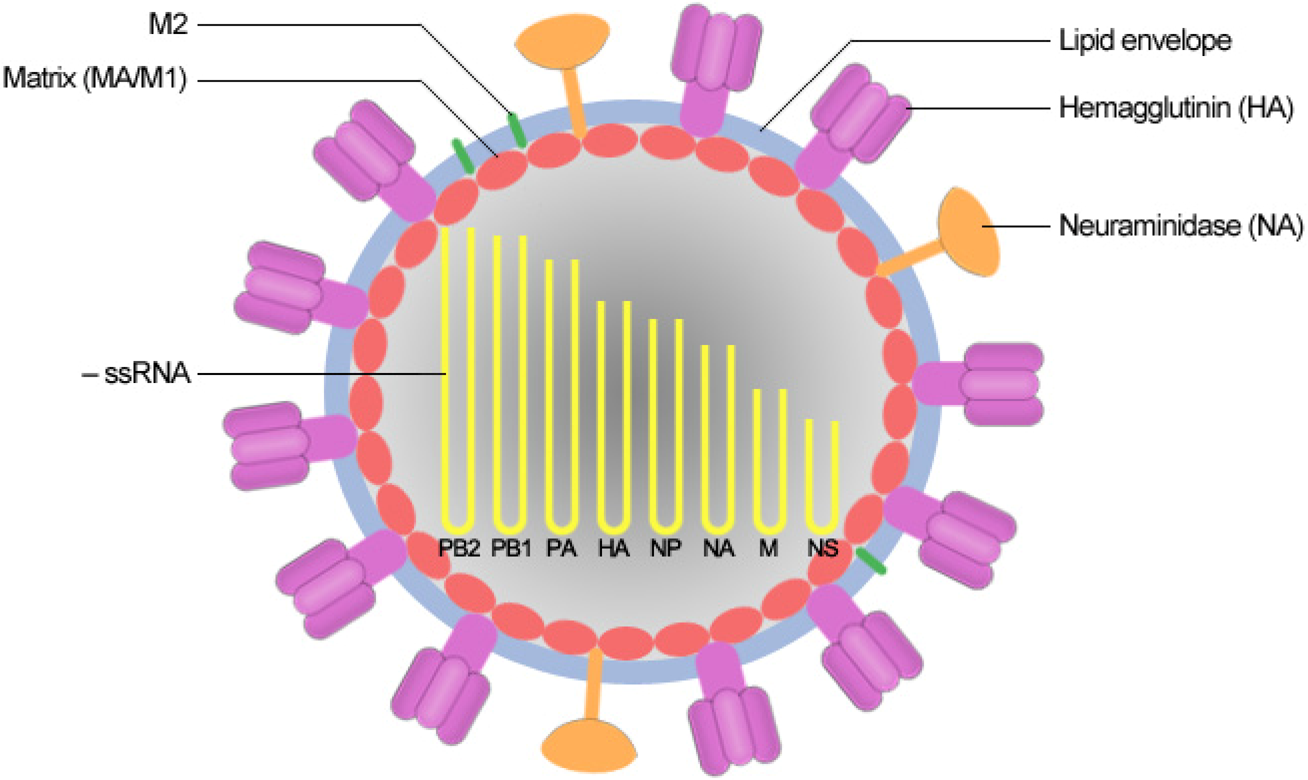
M2
Matrix (MA/M1)
– ssRNA
Lipid envelope
Hemagglutinin (HA)
Neuraminidase (NA)
PB2
PB1
PA
HA
NP
NA
M
NS

A third transmembrane protein, ion channel M2, functions during viral entry and budding [13-15]. Beneath the envelope, matrix protein (MA/M1) gives structure to the virion and acts as a bridge between the ribonucleoprotein core and the lipid envelope [16-18]. The ribonucleoprotein core is a complex of the RNA genome as well as nucleoprotein (NP) and viral polymerase proteins, and lies at the center of the virion. NP binds the genome segments and plays essential roles in replication [19, 20], whereas the viral RNA polymerase proteins (PB1, PB2, PA) are responsible for the transcription and replication of the genome [21, 22]. Three additional proteins are expressed during infection but not included in mature virions: non-structural protein 1 (NS1), which functions to evade host immune responses [23-25]; NS2 (also known as nuclear export protein, or NEP), which mediates the nuclear export of viral genomes [26]; and PB1-F2, which induces cell death in the host [27, 28]. Assembled viral particles are pleomorphic, and can be either spherical with a diameter of ~100 nm [29], or filamentous with dimensions of ~100 nm x 20 μm [30]. Although both forms have been noted in the literature for several decades, the significance of this divergence in morphologies is poorly understood at this time; recent work suggests both forms possess a single copy of the viral genome [31] and are comparably infectious [32].

1.1.2 IVA Genetics

IVA comprises several distinct subtypes based on two antigenic determinants on the viral surface, where isolates are designated a number depending on what variant of the protein is present. This nomenclature is then expressed in the form of H(*n*)N(*n*), where *n* represents the variant of each surface antigen (hemagglutinin, H; neuraminidase, N). As of 2013, there are seventeen H and nine N subtypes, yielding over one hundred and fifty theoretical combinations [33]. Genetic alterations in these subtypes has also necessitated the further classification of strains within subtypes to include information such as the location, year and isolate number of the virus [10].

IVA owes this great variability to its genetic nature. Mutation rates in type B viruses are less than half of those in IVA [34], suggesting that IVA's ability to mutate rapidly is a driving force behind this evolution. Mutations give rise to new strains and subtypes of IVA to which the host immune system is naïve. This strategy effectively subverts immunological memory responses produced by prior infections with other strains and subtypes of the virus [35]. For this reason, humans can become ill from IVA multiple times; this is also the basis for influenza vaccines being administered annually as opposed to a single time. Pandemics can occur if the human population at large has little or no immunity against new viral strains or subtypes resulting from mutations [36]. Mutations are therefore not only significant for viral evolution, but epidemiology as well.

Mutations can arise from two processes: antigenic drift and antigenic shift [37, 38]. Antigenic drift refers to the gradual change in a gene resulting from small changes, such as point mutations, over time. These small mutations in surface antigens can impair recognition by the host's immune system by subtly altering the shape of viral antigens. Antigenic shift is a more dramatic process, involving the exchange of genetic information between two different viruses which have co-infected the same cell [39], a phenomenon facilitated by the segmented nature of the influenza genome. Although far less common than antigenic drift, antigenic shift can result in unpredictable combinations of genes to produce a new virus. A recent example of this was seen in the 2009 pandemic H1N1 virus, which contains genes from avian, swine and human influenza viruses [40]. Fortunately however, the strain lacks mutations known to increase pathogenicity, and the swine-origin antigenic determinants share considerable homology to a virus circulating in humans.

1.1.3 IVA Lifecycle

The lifecycle of IVA begins with receptor binding at the surface of target cells (Figure 2). Using the spike glycoprotein HA, virions bind to sialic acid moieties on the host plasma membrane [41]; airway and respiratory tissues are rich in sialic acid, thus explaining why influenza is a respiratory pathogen [42-44]. Receptor binding triggers the uptake of the virion via endocytosis into an endosome [45, 46]. Following entry, the virion-containing early endosome is trafficked towards the nucleus and matures into a late endosome, an event accompanied by acidification of the compartment [47, 48]. At a sufficiently acidic pH (~5-6), HA undergoes an irreversible conformational change to mediate the fusion of the viral envelope and endosomal membrane, thus releasing the ribonucleoprotein core into the host cytoplasm [49]. Once in the cytoplasm, the core dissociates and the newly freed RNA genome is actively imported into the nucleus, where replication to generate progeny genomes and transcription of mRNAs take place [50-52].

Figure 2 – Overview of the IVA lifecycle

Using the envelope glycoprotein HA, incoming IVA virions bind sialic acid receptors on the surface of host cells, triggering endocytosis. Virion-containing endosomes migrate towards the nucleus becoming increasingly acidic. At a sufficiently low pH, a conformational change in HA triggers the fusion of viral and endosomal membranes, thus releasing the genome-containing ribonucleoprotein core into the host cytosol. After being imported into the nucleus, the viral genome begins replication and mRNA synthesis. While inhibiting host protein synthesis, the virus selectively translates viral proteins in the cytoplasm; transmembrane proteins are translated on rough endoplasmic reticulum. Spike glycoproteins are trafficked through the Golgi and to lipid raft domains in the plasma membrane, where they direct the assembly and release of progeny. The accumulation of viral proteins and genomes progressively increases membrane curvature forming a bud-like structure. M2-mediated scission of viral envelopes and host membrane yields virions with all viral components enclosed. After NA cleaves bonds between virion-associated HA and sialic acid on the host membrane, progeny are released into the extracellular medium.

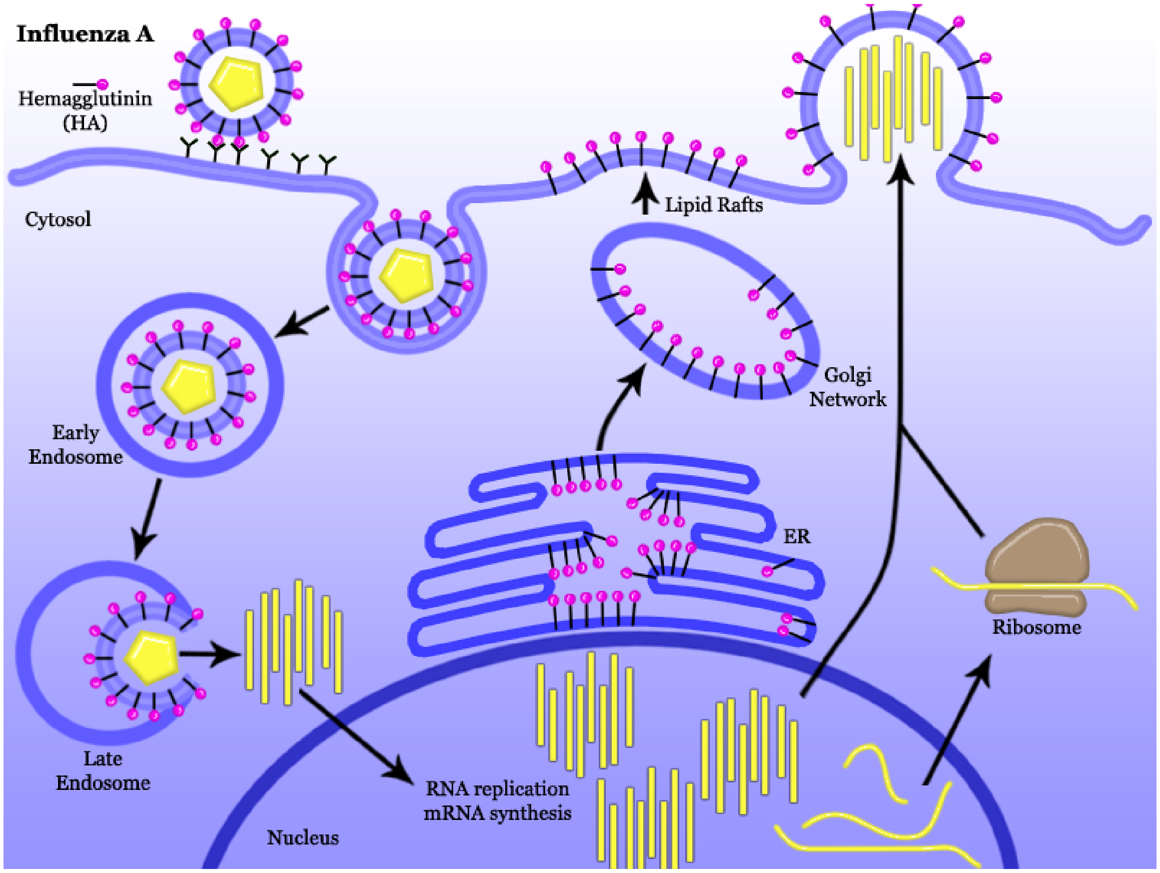
Influenza A
Hemagglutinin (HA)
Cytosol
Lipid Rafts
Golgi Network
Early Endosome
ER
Ribosome
Late Endosome
RNA replication mRNA synthesis
Nucleus

In the nucleus, viral RNA-dependent RNA polymerase initiates the replication of the genome by producing a complementary (+)-sense template in a primer-independent fashion which can then be used in the generation of progeny genomes [53, 54]. Transcription of viral mRNAs begins with the seizure of cellular pre-mRNAs by viral polymerase, which are then catalytically cleaved to liberate their 5' caps. Host-derived 5' caps are then used to prime transcription of viral genes, which end in short poly-U stretches that are repeatedly copied by polymerase, yielding a viral mRNA which bears both a 5' cap and 3' poly-A tail [55, 56]. During this time, the virus orchestrates a number of mechanisms that ensure the preferential translation of viral mRNAs over cellular mRNAs [57]. By blocking host mRNA export from the nucleus [58, 59], host mRNA translation at both initiation and elongation stages [60], and by producing mRNAs which contain sequences that promote their preferential translation [57, 61, 62], the virus both eliminates host protein synthesis and promotes translation of viral proteins [63].

Protein-coding mRNAs are exported from the nucleus to the cytoplasm where they are translated on free ribosomes, or in the case of transmembrane proteins such as HA and NA, on rough endoplasmic reticulum [64]. Following protein synthesis and folding, HA and NA are transported to the plasma membrane via an exocytic pathway, where they are targeted to cholesterol-rich lipid raft microdomains, where progeny virions are assembled and released [65, 66]. Accumulation of HA at the membrane triggers the nuclear export of progeny genomes [67]. The process of nuclear export seems to rely on at least three different viral proteins: NS2/NEP, MA/M1 and NP [68-72]. Once in the cytoplasm, progeny genomes are trafficked independently of membrane proteins using the host cytoskeleton and Rab11-positive recycling endosomes [73-75].

Once at the site of assembly and release, genome segments are packaged in a specific rather than random manner [31, 76, 77]. Although poorly understood at this time, the process of budding and release is thought to begin with deformation of the host membrane, possibly due to HA-induced membrane curvature [78]. The cytoplasmic tails of HA and NA are thought to interact with M1 [79, 80], which subsequently interacts with progeny genomes [17, 81]. This process results in a budding structure which remains connected to the host plasma membrane. For virions to be released from host cells, membrane scission is required to separate the two structures, enclosing ribonucleoprotein complexes in a fully formed viral envelope. Unlike other enveloped viruses, IVA does not utilize host machinery for this process [82-84]; instead, the viral M2 protein mediates the membrane scission of progeny [15, 85]. Although no longer sharing the same membrane, newly formed virions remain attached to the host cell via interactions between HA and sialic acid at the plasma membrane. These bonds are cleaved by NA, allowing virions to be released into the extracellular environment for the next infection cycle [12, 86].

1.1.4 Hemagglutinin

The spike glycoprotein hemagglutinin is an essential component in the IVA lifecycle. HA is the most abundant (~80 %) glycoprotein on the surface of virions [37, 87], and was named in 1941 after its ability to aggregate red blood cells [88]. Unknown at the time, this protein would later be recognized as mediating the binding event which initiates viral entry into a host cell [89]. HA interacts with host sialic acid moieties using a small, highly conserved binding pocket at the outermost tip of the protein [90, 91]. Although the binding affinity of this interaction is weak (K_d ~3 mM), the abundance of virion-associated HA greatly increases its collective avidity, resulting in a tight bond between virion and host cell [92-94].

Following endocytosis, HA is again essential for successful infection, but in a manner completely independent of its receptor binding functions. In addition to triggering the endocytosis of viral particles [45, 46], HA facilitates their escape from endosomes resulting from internalization. As virion-containing endosomes are trafficked from the plasma membrane towards the nucleus, their interior becomes increasingly acidic [95]; paradoxically however, this event is not only advantageous to the virus, but required for its successful entry. When endosomes reach an acidic pH of ~5-6, HA undergoes a conformational change exposing a hydrophobic fusion peptide previously sequestered at neutral pH [96-98]. Insertion of this peptide into the endosomal membrane triggers the fusion of the membrane and viral envelope, forming a pore which allows passage of virion contents to the host cytoplasm [99-101]. Chloroquine, which blocks endosomal acidification, effectively inhibits viral replication by preventing conformational changes in HA and subsequent membrane fusion, underscoring the importance of HA in this process [102].

After mRNA synthesis, HA is synthesized on rough endoplasmic reticulum as a ~75 kDa precursor protein which is transported to the plasma membrane through the Golgi apparatus using host vesicular transport systems [73-75, 103], and is intrinsically targeted to cholesterol-rich lipid raft microdomains in the plasma membrane using sequence determinants [65, 104-107]. Interactions with viral transmembrane proteins serve as scaffolding for the assembly of virions; since HA is the most abundant of these proteins, it has considerable influence in the assembly of progeny [108]. HA accumulation at the membrane serves as a signal to export progeny genomes from the nucleus for packaging into virus particles, a process which also involves HA [67, 109]. Although the importance of HA in the process of budding remains controversial [78, 110], if any virions are released in its absence, they will nonetheless remain non-infectious since HA mediates cell entry.

1.2 Cathepsin B

Cathepsins are a group of proteases found in animal cells which catalyze reactions that degrade proteins. Over a dozen members belong to this family, all of which are distinguished by their structure, function and substrate [111]. Cathepsin B (CTSB) is one such member; a lysosomal cysteine protease coded by the *CTSB* gene, cathepsin B is involved in protein turnover. Over the last two decades however, an increasing body of research has revealed that CTSB plays additional roles in trafficking tumor necrosis factor (TNF)-α containing vesicles [112], NALP3 activation and inflammasome formation [113, 114], and cell death [115]. In light of this, it is perhaps not surprising that CTSB has been implicated in many diseases including arthritis [116], cancer [117] as well as chemotherapy strategies [118, 119], and pancreatitis [120].

1.2.1 Background

CTSB is one of the most abundant lysosomal proteases and is found ubiquitously in eukaryotic cells [121, 122]. It functions as an endopeptidase at neutral pH and an exopeptidase at acidic pH (~5), participating in both early and late stages of endosomal proteolysis [123]. In addition, CTSB has also been found in the cytoplasm [124], at the cell surface [125], and in the nucleus [126]. Apart from degradative roles, CTSB is responsible for the proteolytic cleavage of ricin A [127], soft connective tissue collagen [128], and trypsinogen [129]. Cytosolic release of CTSB is also implicated in multiple cell death pathways by cleaving pro-apoptotic proteins such as Bid, although other mechanisms have also been reported [124, 130-133].

Given the potentially destructive nature of cathepsins, their enzymatic activities are tightly regulated within cells to prevent inadvertent activity. Multiple defence strategies are utilized, including the compartmentalization of cathepsins in organelles, instability at neutral pH, and endogenous inhibitors [134]. Cystatins are a group of cysteine protease inhibitors which serve to prevent the unwanted activity of proteases like CTSB in the cytoplasm or extracellular space [135]. More recently, synthetic inhibitors have proven invaluable tools in research due to their target specificity; the cell-permeable CTSB-inhibitor CA-074 Me (CaMe) is one such highly specific inhibitor [136-139]. However, it should be noted that CaMe also inhibits cathepsin L under reducing conditions [140].

A number of pathologies can result from inappropriate CTSB activity. There is a well-established link between elevated CTSB activity and the metastasis of cancers due to proteolytic degradation of the extracellular matrix and activation of other cascades [141-144]. Similar mechanisms may be the cause of CTSB-mediated joint destruction in the pathology of rheumatoid arthritis [145-148]. On the other hand, impaired CTSB function has been linked to Alzheimer's disease, where CTSB performs a protective role by reducing plaque formation through proteolytic activity [149]. CTSB inhibition has also been shown to impair the lysosomal degradation of lipids, the abnormal accumulation of which can result in atherosclerosis [150].

1.2.2 The role of Cathepsin B in viral lifecycles

Since viruses have a limited coding capacity – some restricted to less than a dozen genes – they are highly economical by nature. As a result, viruses frequently evolve proteins which fulfill multiple functions, or develop cleaver strategies to use host resources. As such, several viruses have found a use for host CTSB in lieu of a virally-encoded factor, though the capacity in which CTSB is utilized in their lifecycles may differ between viruses.

CTSB has been shown to be an essential host factor in the lifecycle of Ebola virus [151]; inhibition of CTSB reduced infection by >90%. Similar to IVA, Ebola virus gains access to cells via endosomes and requires fusion of the viral envelope and the endosomal membrane in order to escape from the endosome into host cytoplasm [152]. To do so, the virus utilizes CTSB to catalytically activate its membrane glycoprotein [153, 154]. Thus, although not required for viral replication [155], CTSB is essential in the process of viral entry. Nipah virus [156], Moloney murine leukemia virus [138], and feline coronavirus [157] use CTSB in a similar fashion.

Unenveloped reovirus does not require CTSB to activate fusion proteins, but instead for the proteolytic disassembly of the viral capsid while in host endosomes [136]. Adeno-associated virus types 2 and 8 use CTSB to cleave capsid proteins, thereby priming rapid disassembly in the nucleus [158]. The catalytic activity of CTSB is also involved in the optimal replication of Herpes simplex virus type I DNA [159]. Additionally, CTSB is required for the proper release of HIV virions from macrophages; when inhibited, virions are retained in intracellular multivesicular bodies and/or endosomes [137]. This study also showed that a CTSB deficiency inhibited the propagation of IVA but not enterovirus, as evidenced by immunofluorescence microscopy using pan-specific antibodies recognizing the respective viruses. Interestingly, it has recently been reported that CTSB is elevated in the plasma and monocytes of HIV-positive individuals, and may be associated with HIV-associated neurocognitive disorders [160].

1.2.3 Potential involvement of Cathepsin B in lipid homeostasis

Although not fully understood at this time, several lines of evidence suggest that CTSB and other members of the cathepsin family play roles in lipid metabolism [161, 162]. This is perhaps best substantiated by the observation that lipids accumulate within cells lacking cathepsins such as CTSB as a result of impaired lipid metabolism [163]. Not surprisingly, this intracellular accumulation of lipids has implicated CTSB in the pathology of atherosclerosis, a condition characterized by the progressive thickening of arterial walls due to the accumulation of fatty deposits.

Interestingly, cathepsin D has been shown to be involved in the transport of endocytosed cholesterol from intracellular compartments to the plasma membrane [164, 165]. Inhibition of CTSD reduces the transcription of the cholesterol transporter ABCA1, thereby reducing cholesterol transport by 70%. This results in the accumulation of lipids within endosomes, closely resembling the phenotype of the lysosomal storage disorder Niemann-Pick disease type C (NPC); NPC is a consequence of mutations to the *NPC1* gene, which codes for a cholesterol transporter [165-169]. Thus, it is possible that the documented observations of CTSB-dependent lipid accumulation might function through similar means by altering the expression of cholesterol transporters.

1.3 Rationale, hypothesis and objectives

CTSB is a lysosomal protease involved in the lifecycles of some viruses. Recent work from our lab showed that CTSB is required for HIV-1 virus-like particle release, and possibly the propagation of herpes simplex virus 1 (HSV-1) and IVA [137]. Based on these observations, I hypothesize that CTSB is required for the optimal replication and/or release of influenza virions. Given the various roles of CTSB in the lifecycles of other viruses, it was pertinent to address this hypothesis by assessing whether a CTSB-deficiency – either genetic or pharmacological – had any effect on different stages in the IVA lifecycle. By examining viral entry, replication, HA protein production, trafficking of HA to the plasma membrane, and release of viral particles in CTSB-deficient cells or cells treated with the CTSB inhibitor CaMe, I attempted to elucidate which of these processes, if any, relied on CTSB.

Chapter 2: Methods

2.1 Reagents

The synthetic CTSB inhibitor [L-3-trans-(Propylcarbamoyl)oxirane-2-carbonyl]-L-isoleucyl-L-proline Methyl Ester (CA-074 Me; CaMe) was purchased from Peptide Institute Inc. (Osaka, Japan). Actinomycin D (ActD; A9415) and LysoTracker Red (L-7528) were purchased from Sigma (Oakville, Canada). Influenza A H1N1/Puerto Rico/8/34 (PR8) was obtained from Dr. Mansour Haeryfar (London, Canada).

Primary antibodies used included anti-β Actin (rabbit; Rockland #600-401-886) and anti-HA (mouse; sterile culture supernatant of monoclonal hybridoma H28-E23; a kind gift from Dr. Mansour Haeryfar; London, Canada). Secondary antibodies used included goat anti-rabbit IgG IRDye 800 (Li-Cor #926-32211; Lincon, United States), goat anti-mouse IgG IRDye 800 (Li-Cor #926-32210; Lincon, United States), and fluorescein-conjugated $F(ab')_2$ fragment goat anti-mouse IgG (Jackson ImmunoResearch #115-096-146; West Grove, United States).

2.2 Cell Culture

Human lung adenocarcinoma (A549) cells were grown in DMEM supplemented with 10% heat-inactivated fetal bovine serum (FBS; VWR; Mississauga, Canada), 1 mM MEM non-essential amino acid solution, 100 U/mL penicillin G, 100 μg/mL streptomycin and 1 mM sodium pyruvate (Sigma; Oakville, Canada).

Bone marrow-derived immortalized macrophages (BMDIM) from C57 BL/6 mice were prepared from wildtype (Wt) or $CTSB^{-/-}$ (KO) backgrounds as described previously [112, 170]. C57 cells were grown in RPMI 1640 supplemented with 10% heat-inactivated fetal bovine serum (FBS; Sigma; Oakville, Canada), 1 mM MEM non-essential amino acid solution, 100 U/mL penicillin G, 100 μg/mL streptomycin and 1 mM sodium pyruvate.

All cells were grown at 37˚C in a humidified atmosphere containing 5% CO_2.

2.3 Viral Infections

One million cells were placed in 15 mL conical tubes and infected with PR8 at an MOI of 1, 5 or 10 (depending on the experiment) for one hour in 1 mL of PBS rotating at 37˚C. Conditions with CaMe or ActD received the drug at the time of infection. After one hour adsorbtion, 5 mL of complete culture medium was added to the cells (with drug, if applicable) and incubation continued for a further 5 hours while rotating at 37˚C.

2.4 Western Blot

Samples were lysed on ice for 20 minutes in cold lysis buffer (50 mM tris-HCl [pH=7.4], 150 mM NaCl, 1 mM EDTA, 1% Triton X-100, 0.1% SDS with protease inhibitor cocktail [Roche; Mississauga, Canada]) and run on 10% SDS gels at a voltage of 110V for 1.5 hours. Following this, the gel was semi-dry transferred onto PVDF (Pall Life Sciences #BSP0161; Mississauga, Canada) for 1.5 hours at 18V. Membranes were blocked in 5% (w/v) skim milk in tris-buffered saline (TBS; 50 mM tris-HCl, 150 mM NaCl, pH 7.5) containing 0.08% Tween 20 (TTBS) for one hour and probed with primary antibodies at a 1:1000 dilution in TTBS overnight at room temperature. The following day, blots were washed in TTBS and incubated with secondary antibodies at a dilution of 1:10000 in TTBS for one hour. Blots were imaged using the Li-Cor Odyssey system (Guelph, Canada).

Densitometric analysis on Western blots was performed using the densitometry feature in ImageJ (NIH; Bethesda, United States). Lanes were analyzed and the resulting histograms were used to measure band density by measuring the area under each peak with any background subtracted. Densities of target immunoreactivities were then normalized to a loading control (β-actin) for data analysis.

2.5 RT-qPCR

Briefly, RNA was extracted from cells using TriZol (Invitrogen; Burlington, Canada) and 0.5 µg was reverse transcribed with M-MuLV (New England Biolabs; Whitby, Canada) following manufacturer's protocols using two viral gene-specific primers to yield template cDNA (see below). One µL of this sample was amplified with SYBR Green PCR Master Mix (Invitrogen; Burlington, Canada) and quantified using a Rotor-Gene RG3000 (Corbett

Life Science; Kirkland, Canada) with the following cycling conditions: 94˚C for 2 min; 94˚C for 15 sec, 54˚C for 30 sec, and 72˚C for 30 sec with 30 cycles. Target amplicons for the two genes were PCR-amplified and a standard curve of each was generated by making a series of ten-fold dilutions (Figure 3). Known concentrations of amplicon were used to calculate copy number, and the resulting equations were used to determine the copy numbers of unknown samples based on Ct values as described previously [171, 172].

HA primers were generated from a sequence specific to the PR8 strain of influenza (GenBank: CY009447.1) using Primer3.

HA Fwd/RT primer: 5'-TGCTTCAAAACAGCCAAGTG-3'

HA Rev primer: 5'-GCCCAGTACCTGCTTCTCAG-3'

MA primers were generated from a sequence reported in literature to be highly conserved among viral subtypes [173].

Matrix Fwd/RT primer: 5′-CTTCTAACCGAGGTCGAAACG-3′

Matrix Rev primer: 5'- GCATTTTGGACAAAGCGTCT-3'

2.6 Fractionation

Crude and purified lysosome/endosome fractions were obtained using a lysosome isolation kit (Sigma; Oakville, Canada). Briefly, 3 x 10^7 C57 cells were lysed using a Dounce homogenizer as directed. Nuclei and debris were pelleted by centrifugation for 10 min at 1000 g, and organelles (mitochondria, lysosomes, peroxisomes, endoplasmic reticulum, late endosomes) were isolated from the resulting supernatant by centrifugation for 20 min at 20000 g to yield the crude fraction. A proportion of this fraction was further purified by adding 8 mM calcium chloride and centrifuging for 15 min at 5000 g to yield a purified fraction of late endosomes/lysosomes. These fractions were then assayed for their cholesterol and protein contents as described below.

2.7 Cholesterol Assay

Lipids were extracted from lysed cells from Section 2.6 using the Folch method [174, 175]. Briefly, cell lysates were added to a 2:1 chloroform-methanol solution and lipids were extracted by vacuum drying the organic phase. Cholesterol content was assayed using the Amplex Red Cholesterol Assay Kit (Invitrogen #A12216; Burlington, Canada) following manufacturer's instructions.

2.8 Protein Assay

Protein assays were done in tandem with cholesterol assays using a fraction of cell lysates prepared for the cholesterol assay (above). Protein concentration was determined using Bradford reagent (BioRad; #500-0006; Mississauga, Canada) following manufacturer's directions of the Bradford technique [176]. A BSA reference curve was generated with each replicate to give a standard curve of protein concentrations that was used to determine the concentration of samples.

2.9 Immunofluorescence Microscopy

Fifty thousand A549 cells suspended in 50 μL of PBS were seeded onto coverslips and allowed to attach (~1 hour). Cells were then infected with PR8 at a high MOI (5 or ~10) by directly pipetting virus onto coverslips; any inhibitors indicated were added at this time. After a one hour adsorbtion period, 2 mL of warm media (with inhibitors, if applicable) was added to 6-wells containing coverslips and incubation was allowed to continue for an additional 4.5 hours. At this point, LysoTracker Red was added to a final concentration of 200 nM and coverslips were allowed to incubate for 30 min. After the six hour infection period was complete, coverslips were washed in PBS and fixed in 4% formaldehyde for 17 min. For conditions requiring permeabilization, cells were treated with 0.25% Triton X-100 for 10 min. After two washes in PBS, coverslips were blocked in PBS + 1% BSA + 0.05% Tween 20 for one hour and then incubated in anti-HA primary antibody at a 1:10 dilution overnight at 4˚C. The following day, slides were washed in PBS and incubated in secondary (anti-mouse FITC) at a 1:100 dilution for two hours. Slides were then washed once more and incubated in Hoechst 33342 for 3 min at a 1:4000 dilution, rinsed, mounted, and viewed using a Bio-Rad Radiance 2000 fluorescence microscope or a Zeiss LSM 510 confocal fluorescence microscope. Images were acquired using QCapture Pro 6.0 (QImaging; Surrey, Canada) or Zen 2008 (Zeiss; Toronto, Canada) for the Bio-Rad Radiance 2000 and Zeiss LSM 510, respectively. Colocalization was assessed using the JACoP plugin for ImageJ [177].

2.10 Hemagglutination Assay

Hemagglutination assays were performed as described previously [178]. Briefly, 1 x 10^6 A549 cells were infected at an MOI of 1 in the presence or absence of CaMe (150 or 500 µM) in a total volume of 1 mL PBS. After one hour adsorption, PBS and virus were aspirated, and cells were washed twice in PBS. Two mL of fresh serum-free DMEM with 2.5 µg/mL trypsin was added, along with CaMe if applicable, and incubation continued for an additional 23 h. Twenty four hours post-infection, supernatant was collected and centrifuged to pellet debris. Fifty µL from each condition was added to 50 µL of PBS in triplicate and serially diluted two-fold. A PBS-only control and a positive control using the stock virus were run with each replicate. Fifty µL of a 0.5% adult chicken erythrocyte (Charles River Laboratories; Wilmington, United States) solution in PBS was added to each well and gently mixed. After incubating 30 min at room temperature, wells were scored as either positive or negative, and the titre reported as the reciprocal of the highest dilution which yielded agglutination.

2.11 MTT Assay

Seventy five thousand cells in triplicate 96-wells were treated in the presence or absence of drug for six hours at 37˚C to reproduce conditions during infection. After treatment, MTT was added to a final concentration of 0.5 mg/mL and incubation continued for an additional 2 hours. When incubation was complete, culture medium was aspirated and 100 µL of DMSO was added to solubilize cells and dye. After a 10 min incubation, absorbance was read at 570 nm using a plate reader, and the values of blank wells were averaged and subtracted from samples. Untreated conditions served as positive controls from which viability was calculated.

2.12 Statistical Analysis

Statistical analysis was performed using GraphPad Prism 4 (GraphPad Software; San Diego, United States). Results were considered statistically significant if $p \leq 0.05$ for either t-test or one-way ANOVA followed by a Tukey's post hoc test, as stated in the figure legend. Data are presented as means ± SEM, where error bars denote biological variations between experiments. Colocalization was assessed using the JACoP plugin for ImageJ to determine Pearson's coefficients to numerically define the degree of overlap between red and green channels.

Chapter 3: Results

3.1 The role of CTSB in influenza A virus entry and replication

Recent work in our lab identified CTSB as a requirement for HIV release and the propagation of IVA [137]. Additionally, CTSB has been shown to be indispensable in the lifecycles of other viruses [136, 138, 151, 153, 154, 156-158]. The majority of these viruses require the catalytic activity of CTSB to activate proteins used for entry into the cell or escape from endocytic compartments post-internalization. To assess the role of CTSB on the entry and replication of IVA, cells with and without functional CTSB were infected in the presence or absence of an IVA replication inhibitor (Actinomycin D; ActD), which facilitates discrimination between virions from the inoculum and those produced via replication. For this purpose, two cell lines were selected: CTSB$^{+/+}$ (Wt) and CTSB$^{-/-}$ (KO) C57 BMDIM, as well as A549 human lung adenocarcinoma cells with and without the CTSB inhibitor CA-074 Me (CaMe). Total RNA was harvested from infected cell lysates and the extent of viral entry and replication was determined by measuring the concentration of viral genes using RT-qPCR.

IVA genes are packaged in equal quantities, with a single copy of each per virion [179, 180]. Therefore, since copy numbers between genes are expected to be similar, two viral genes were quantified for each sample to enhance the validity of these measurements: a region of the hemagglutinin (HA) gene specific to the PR8 strain of IVA, and a region in the matrix (MA) gene reported to be highly conserved among IVA subtypes [173].

To convert Ct values obtained from RT-qPCR into copy numbers for each gene, a reference containing known concentrations of each amplicon was generated. Amplicons for each gene were PCR amplified from infected cells using respective primers. Gel-purified amplicons were then quantitated using spectrophotometry, serially diluted ten-fold, and subjected to qPCR as described in Section 2.5. Ct values were plotted against the concentration of each dilution and the equation generated from a trendline was used to calculate the concentration of unknown samples on the basis of Ct values (Figure 3). Using the known size of each amplicon, the concentration could then be converted into the copy number of that gene.

Figure 3 – Standard curves of qPCR Ct values for known concentrations of amplicon.

Gel-purified PCR amplicons generated from HA and MA primer pairs (top) were quantified and serially diluted ten-fold. The dilution series was then subjected to qPCR as described in "Methods" to obtain Ct values corresponding to the amplicon concentration (bottom). The concentration and subsequently the copy number of each viral gene was calculated using the equations generated by the standard curves. Both primer pairs had efficiencies greater than 99%.

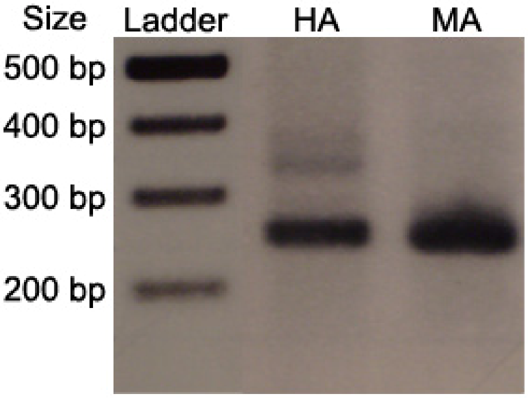
Size
Ladder
HA
MA
500 bp
400 bp
300 bp
200 bp

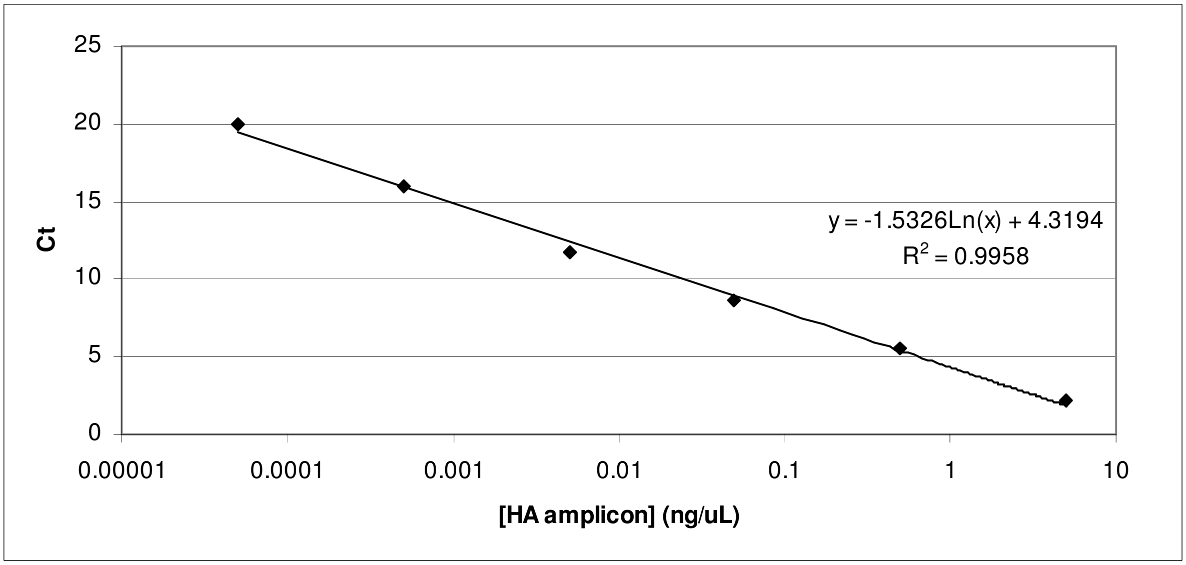
25
20
15
10
5
0
Ct
0.00001
0.0001
0.001
0.01
0.1
1
10
[HA amplicon] (ng/uL)
y = -1.5326Ln(x) + 4.3194
R² = 0.9958

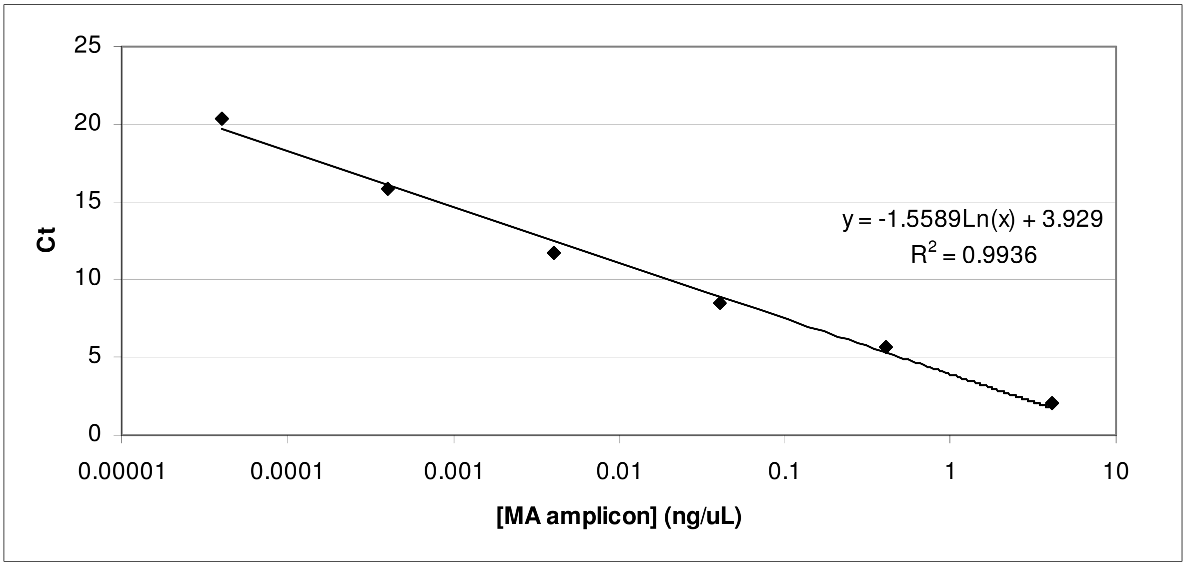
25
20
15
10
5
0
Ct
0.00001
0.0001
0.001
0.01
0.1
1
10
[MA amplicon] (ng/uL)
y = -1.5589Ln(x) + 3.929
R² = 0.9936

3.1.1 CTSB is not required for influenza virus entry and replication in BMDIM cells

Since genetic knockouts are considered the gold standard for assessing the function of a gene, initial experiments employed the use of a murine CTSB knockout cell line previously generated in the lab [137].

As shown in Figure 4, copy numbers of HA and MA were not significantly different between Wt and KO cells in the presence or absence of ActD. ActD treatment showed no significant differences in viability between Wt and KO cells (Figure 5A). As expected, copy numbers of HA and MA genes closely resembled each other, with the exception of untreated KO cells.

3.1.2 CTSB is not required for influenza virus entry and replication in A549 cells

In addition to using a knockout cell line, these findings were then assessed using a more physiologically relevant cell type: A549 human lung adenocarcinoma cells. A549 cells more closely approximate the respiratory epithelium which is infected *in vivo*, and as such are commonly used in influenza research [181-186]. Since a knockout in this cell line was unavailable, CTSB was pharmacologically inhibited using the cell-permeable drug CaMe [136-139].

As shown in Figure 6, there were no significant differences in HA or MA copy numbers between untreated cells (0 μM) and cells treated with different concentrations of CaMe, both in the presence and absence of ActD. ActD treatment showed no significant difference in cell viability (Figure 5B). As expected, copy numbers of HA and MA closely resembled each other for all samples.

3.2 The role of CTSB in viral HA protein production

Since CTSB was involved in neither viral entry nor replication, the next stage in the viral lifecycle, protein synthesis, was examined. To this end, cell lysates of IVA-infected C57 Wt and KO cells, as well as A549 cells in the presence or absence of CaMe, were subjected to Western blotting for viral HA protein. Densitometric analysis of the immunoreactive bands was performed and the intensities were normalized to those of β-actin.

Figure 4 – Viral entry and replication are not significantly different between wildtype and CTSB$^{-/-}$ cells.

BMDIM from C57BL/6j mice either with (Wt) or lacking (KO) a functional CTSB gene were infected with influenza A virus strain PR8 for six hours at an MOI of 1 in the presence or absence of actinomycin D (ActD; 5 µg/mL), a transcription inhibitor. Following infection, cells were harvested and extracted RNA was used as a template for qPCR reactions using virus-specific primers for hemagglutinin (HA; PR8-specific) and matrix protein (MA; pan-specific). ActD is a potent inhibitor of influenza virus replication, and therefore this treatment allows for the detection of incoming viral RNA while excluding that generated during infection. A standard curve of purified template was used to generate copy numbers for each gene (Figure 3); since viral genes are packaged at a 1:1 ratio, copy numbers of HA and MA are directly correlated, and are indicative of the number of viral particles present. (**A&B**) There were no significant differences ($p > 0.05$; one-way ANOVA) in copy number between Wt and KO cells in viral endocytosis (ActD+) or viral replication (ActD-) for either the HA (A) or MA (B) gene ($n \geq 3$). Data are expressed as means ± SEM from at least three independent experiments. Columns accompanied by the same letter are not significantly different from each other by Tukey's post hoc test.

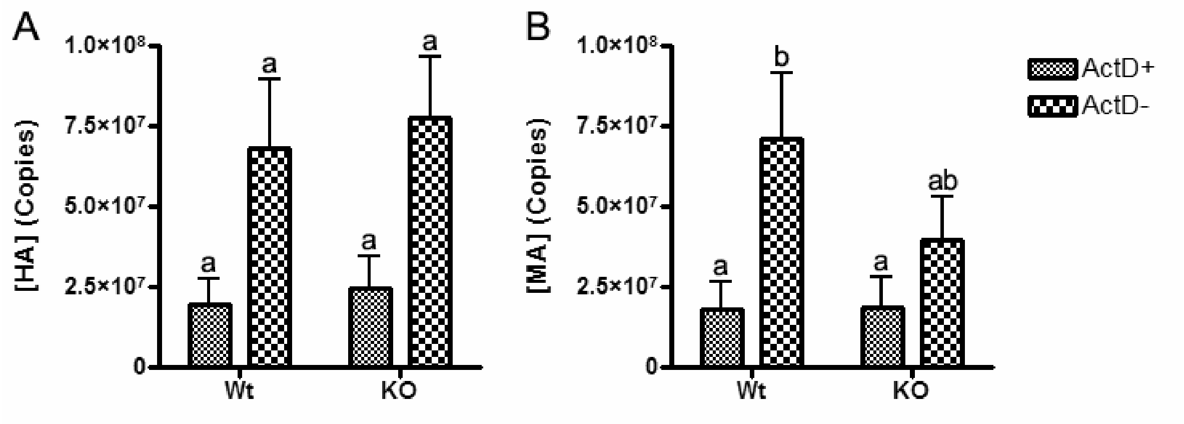
A
B
1.0×10⁸
7.5×10⁷
5.0×10⁷
2.5×10⁷
0
[HA] (Copies)
[MA] (Copies)
Wt
KO
a
b
ab
ActD+
ActD-

Figure 5 – Toxicity of ActD in C57 and A549 cells.

Wt and KO C57 cells (A) and A549 cells (B) were treated in the presence or absence of 5 μg/mL ActD for six hours, emulating the conditions used in this study. After incubation, an MTT assay was performed and the cell death measured. (**A&B**) No significant differences in cell death were detected between Wt and KO cells, nor between treated and untreated A549 cells ($p > 0.05$; t-test; n=3). Data are expressed as means ± SEM. N.S. = not significant.

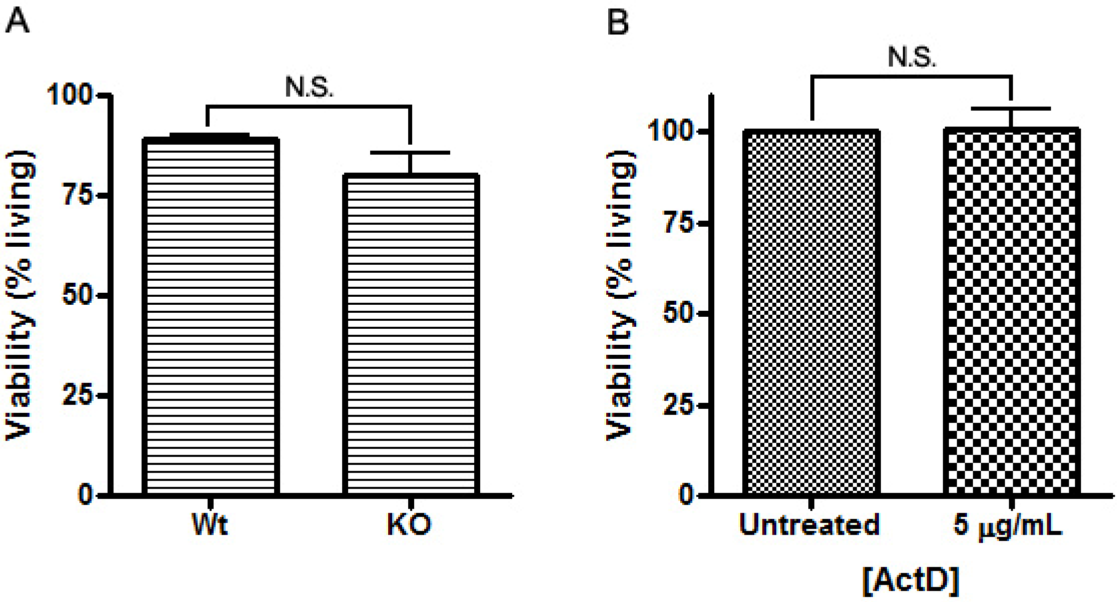
A
N.S.
Viability (% living)
100
75
50
25
0
Wt
KO
B
N.S.
Viability (% living)
100
75
50
25
0
Untreated
5 μg/mL
[ActD]

Figure 6 – Viral entry and replication are not significantly different in CaMe-treated A549 cells.

A549 lung adenocarcinoma cells treated with different concentrations of the CTSB inhibitor CaMe were infected with influenza A virus strain PR8 for six hours at an MOI of 1 in the presence or absence of actinomycin D (ActD; 5 µg/mL), a transcription inhibitor. Following infection, cells were harvested and extracted RNA was used as a template for qPCR reactions using virus-specific primers for hemagglutinin (HA; PR8-specific) and matrix protein (MA; pan-specific). Actinomycin D is a potent inhibitor of influenza virus replication, and therefore this treatment allows for the detection of incoming viral RNA while excluding that generated during infection. A standard curve of purified template was used to generate copy numbers for each gene (Figure 3); since viral genes are packaged at a 1:1 ratio, copy numbers of HA and MA are directly correlated, and are indicative of the number of viral particles present. (**A&B**) There were no significant differences ($p > 0.05$; one-way ANOVA) in copy number between untreated A549 cells and any of the tested concentrations of CaMe for either the HA (A) or the MA (B) gene in the presence or absence of ActD ($n \geq 3$). Data are expressed as means ± SEM from at least three independent experiments. Columns accompanied by the same letter are not significantly different from each other by Tukey's post hoc test.

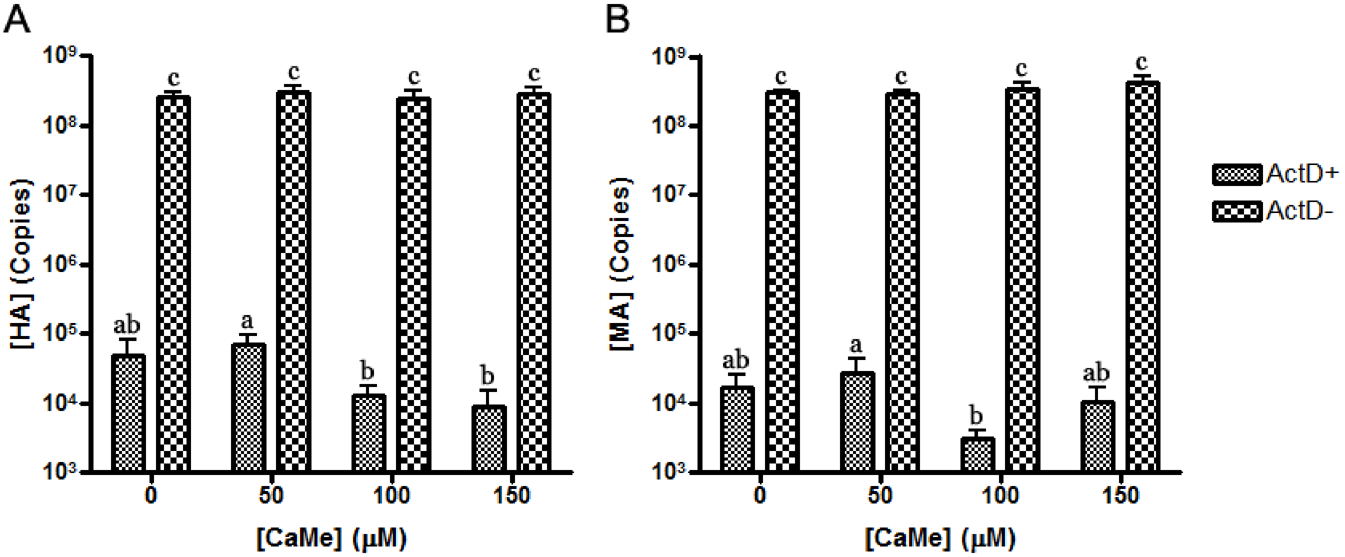
A
B
[HA] (Copies)
[MA] (Copies)
10⁹
10⁸
10⁷
10⁶
10⁵
10⁴
10³
0
50
100
150
[CaMe] (μM)
ab
a
b
b
ab
a
b
ab
c
ActD+
ActD-

3.2.1 A deficiency in CTSB reduces viral HA protein production in BMDIM cells

Since there were no significant differences in viral entry or replication, I next investigated whether protein production was defective. As shown in Figure 7, the amount of viral HA protein detected in the lysates of infected KO cells was significantly reduced relative to Wt cells. Similar results were also obtained using primary cells from mice of the same genotypes used to generate the cell lines (Figure 8).

3.2.2 A deficiency in CTSB reduces viral HA protein production in A549 cells

Viral HA protein production was also assessed in A549 cells treated with different concentrations of CaMe. Similar to findings obtained in the KO cell line, 150 μM CaMe treatment significantly reduced HA protein levels compared to untreated cells (Figure 9B). A vehicle control showed no differences in HA protein compared to untreated cells (Figure 10). CaMe treated cells showed no significant differences in viability compared with untreated controls (Figure 11).

3.3 Pharmacological inhibition of CTSB reduces surface expression of HA protein on infected cells

After synthesis, HA is trafficked to the host plasma membrane via the Golgi network where it is embedded on the cell surface [87]. Since CTSB inhibition or deficiency reduced HA protein levels in infected cells, it was important to investigate whether transport of HA to the cell surface was impacted. To this end, A549 cells were infected in the presence or absence of either CaMe or ActD, stained for viral HA and examined by either immunofluorescence (Figure 12A) or confocal microscopy (Figure 12B-D).

As shown in Figure 12A, infection of untreated cells yielded a diffuse staining pattern for HA (green) across the cell. Treatment with 5 μg/mL ActD abolished this staining, and instead only sparse puncta were visible. Similarly, cells infected in the presence of 150 μM CaMe showed puncta upon staining as well.

Figure 7 – CTSB$^{-/-}$ cells produce significantly less viral HA protein.

BMDIM from C57BL/6j mice either with (Wt) or lacking (KO) a functional CTSB gene were infected with influenza A virus strain PR8 for six hours at an MOI of 1. Following infection, cells were harvested, lysed and subjected to Western blotting for the influenza HA protein, and the resulting blots were used for densitometric analysis to express the density of HA normalized to actin. (**A**) A representative Western blot for HA protein in cell lysates. (**B**) Infected KO cells had significantly less ($p = 0.05$; t-test) HA protein compared to Wt cells ($n=3$). Data are expressed as means ± SEM from three independent experiments.

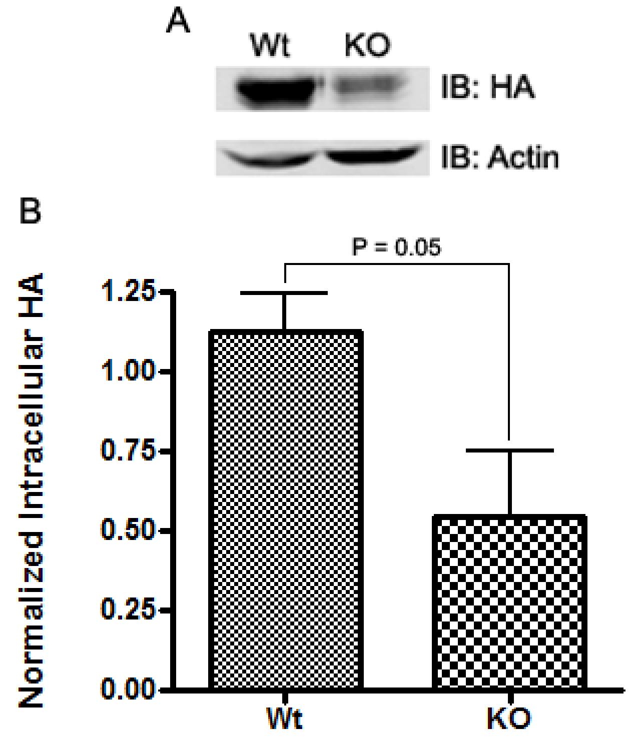
A
Wt
KO
IB: HA
IB: Actin
B
P = 0.05
Normalized Intracellular HA
1.25
1.00
0.75
0.50
0.25
0.00
Wt
KO

Figure 8 – Primary CTSB$^{-/-}$ cells produce less viral HA protein compared with Wt.

Monocyte-derived macrophages from the bone marrow of C57 mice either with (Wt) or lacking (KO) a functional CTSB gene were infected with influenza A virus strain PR8 (+) for six hours at an MOI of 1. Uninfected controls (-) from both the 6 h and 0 h time points were also collected for each cell type. Following infection, cells were harvested, lysed and subjected to Western blotting for the influenza HA protein. KO cells showed less HA protein compared to Wt (n=2).

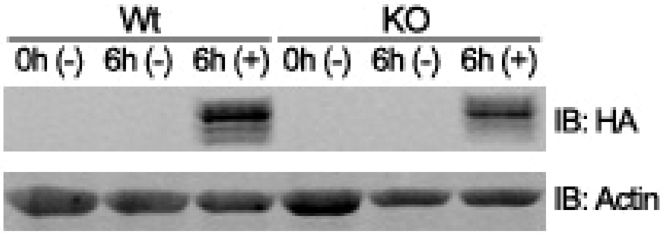
Wt
KO
0h (-)
6h (-)
6h (+)
0h (-)
6h (-)
6h (+)
IB: HA
IB: Actin

Figure 9 – A549 cells treated with 150 µM CaMe produce significantly less viral HA protein.

A549 lung adenocarcinoma cells treated with different concentrations of the CTSB inhibitor CaMe were infected with influenza A virus strain PR8 for six hours at an MOI of 1. Following infection, cells were harvested, lysed and subjected to Western blotting for the influenza HA protein, and the resulting blots were used for densitometric analysis to express the density of HA normalized to actin. (**A**) A representative Western blot for HA protein in cell lysates. (**B**) A549 cells treated with 150 µM CaMe showed significantly less ($p < 0.05$; one-way ANOVA) HA protein compared to untreated controls (n=4). Data are expressed as means ± SEM from four independent experiments. Columns accompanied by the same letter are not significantly different from each other by Tukey's post hoc test.

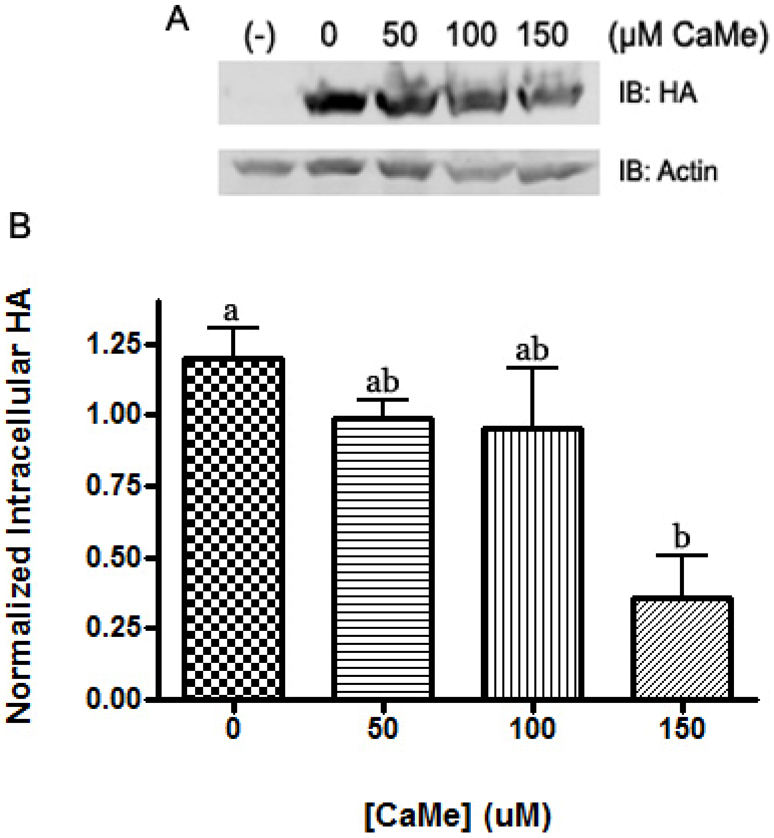
A
(-)
0
50
100
150
(μM CaMe)
IB: HA
IB: Actin
B
Normalized Intracellular HA
1.25
1.00
0.75
0.50
0.25
0.00
a
ab
ab
b
0
50
100
150
[CaMe] (uM)

Figure 10 – Vehicle control for CaMe treatment of A549 cells.

A549 cells were infected with PR8 (+) at an MOI of 1 in the presence or absence of DMSO equivalent to 150 μM CaMe treatment as described in Methods. An uninfected control (-) received PBS instead of virus. After six hours, cells were washed and lysates were probed for viral HA protein contents and β-actin by Western blotting.

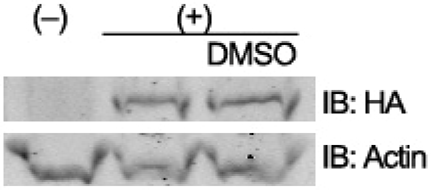
(–)
(+)
DMSO
IB: HA
IB: Actin

Figure 11 – Toxicity of CaMe in A549 cells.

A549 cells were treated in the presence or absence of CaMe at the concentrations used in this study for six hours. After incubation, an MTT assay was performed and the cell death measured. No significant cell death was detected for any treatments ($p > 0.05$; one-way ANOVA; n=3). Data are expressed as means ± SEM. Columns accompanied by the same letter are not significantly different from each other by Tukey's post hoc test.

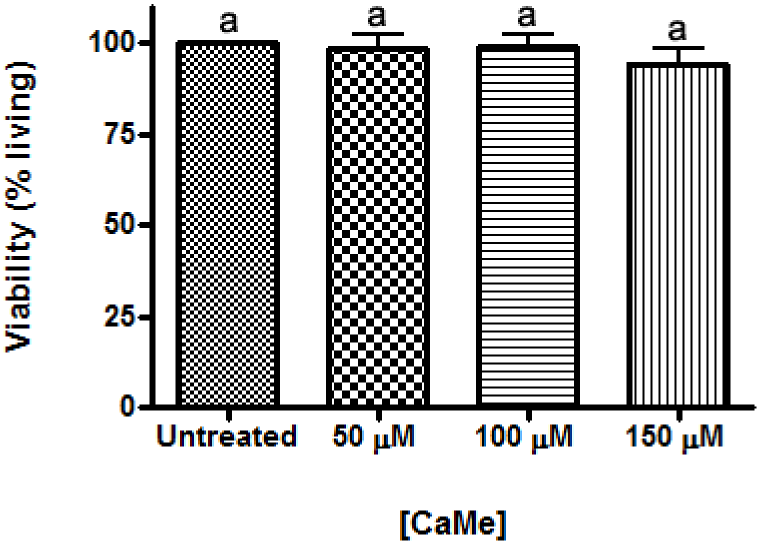
Viability (% living)
100
75
50
25
0
a
a
a
a
Untreated
50 µM
100 µM
150 µM
[CaMe]

Figure 12 – Inhibition of CTSB in A549 cells with 150 µM CaMe reduces surface expression of HA protein.

Coverslips with adherent A549 cells were infected for six hours at a high MOI (>10) in the presence of PBS (A top left, B), CaMe (150 µM; A top right, C), ActD (5 µg/mL; A bottom left, D) or CaMe and ActD (A lower right). At 5.5 h, LysoTracker Red was added to a final concentration of 200 nM and allowed to incubate for 30 min. At 6 h, coverslips were removed from virus-containing medium, fixed in 4% formaldehyde, and blocked in PBS + 1% BSA + 0.05% Tween 20 for 1 h. Coverslips were then incubated in anti-HA primary antibody at a 1:10 dilution overnight at 4˚C. The following day, slides were washed in PBS and incubated in secondary (anti-mouse FITC) at a 1:100 dilution for 2 h. Slides were then washed once more and incubated in Hoechst 33342 for 3 min at a 1:4000 dilution, rinsed, mounted, and viewed using a Bio-Rad Radiance 2000 fluorescence microscope (A) or a Zeiss LSM 510 confocal fluorescence microscope (B-D). Images shown are representative cells from respective treatments from three independent experiments. (**A**) Untreated cells showed diffuse staining for HA (green) across the cell surface. Cells treated with either CaMe or ActD showed no such staining, and instead showed puncta on the surface of the cell. (**B**) Untreated cells showed diffuse staining for HA (green) across the cell membrane. (**C&D**) Cells treated with either CaMe (C) or ActD (D) showed no such staining, and instead showed puncta on the cell periphery.

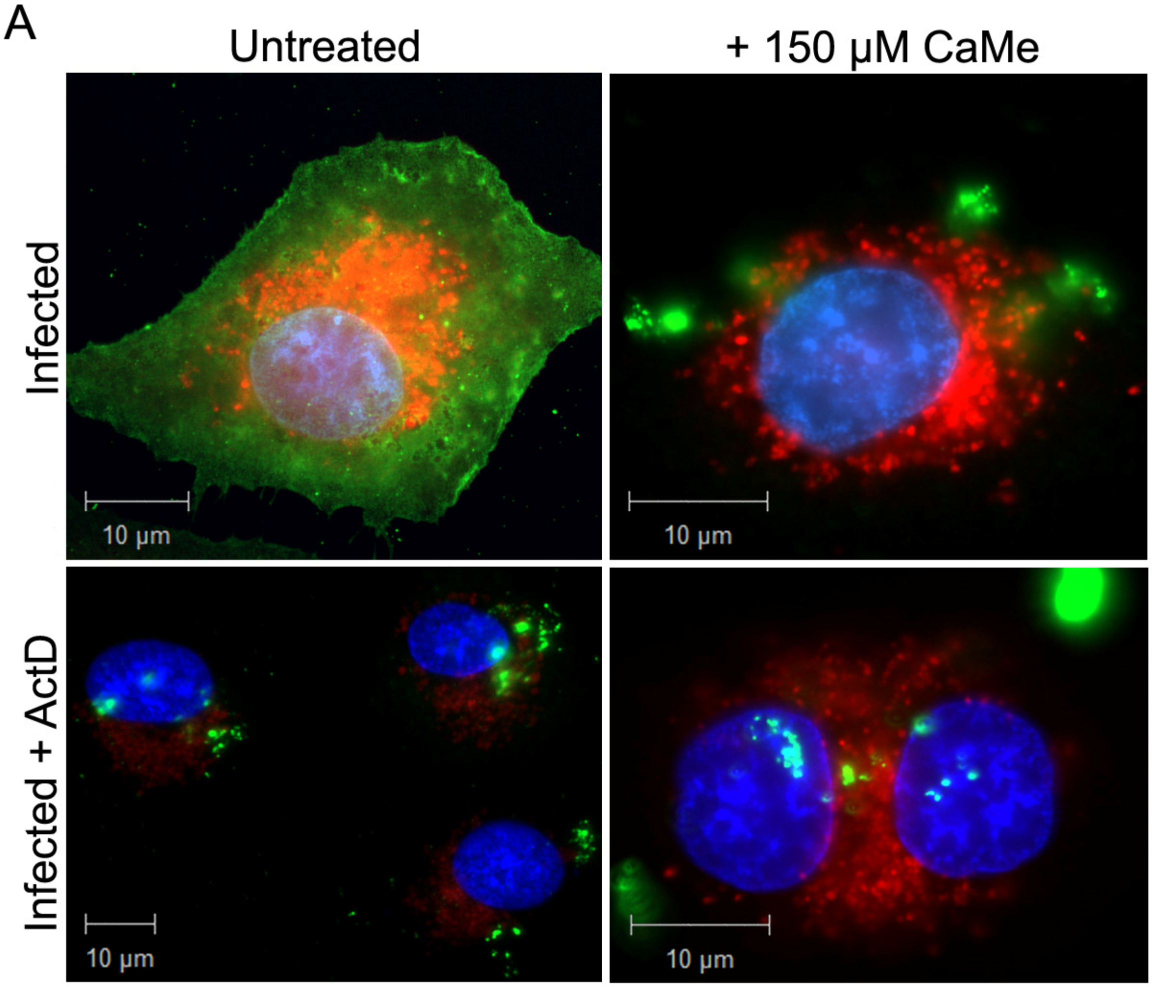
A
Untreated
+ 150 µM CaMe
Infected
Infected + ActD
10 µm
10 µm
10 µm
10 µm

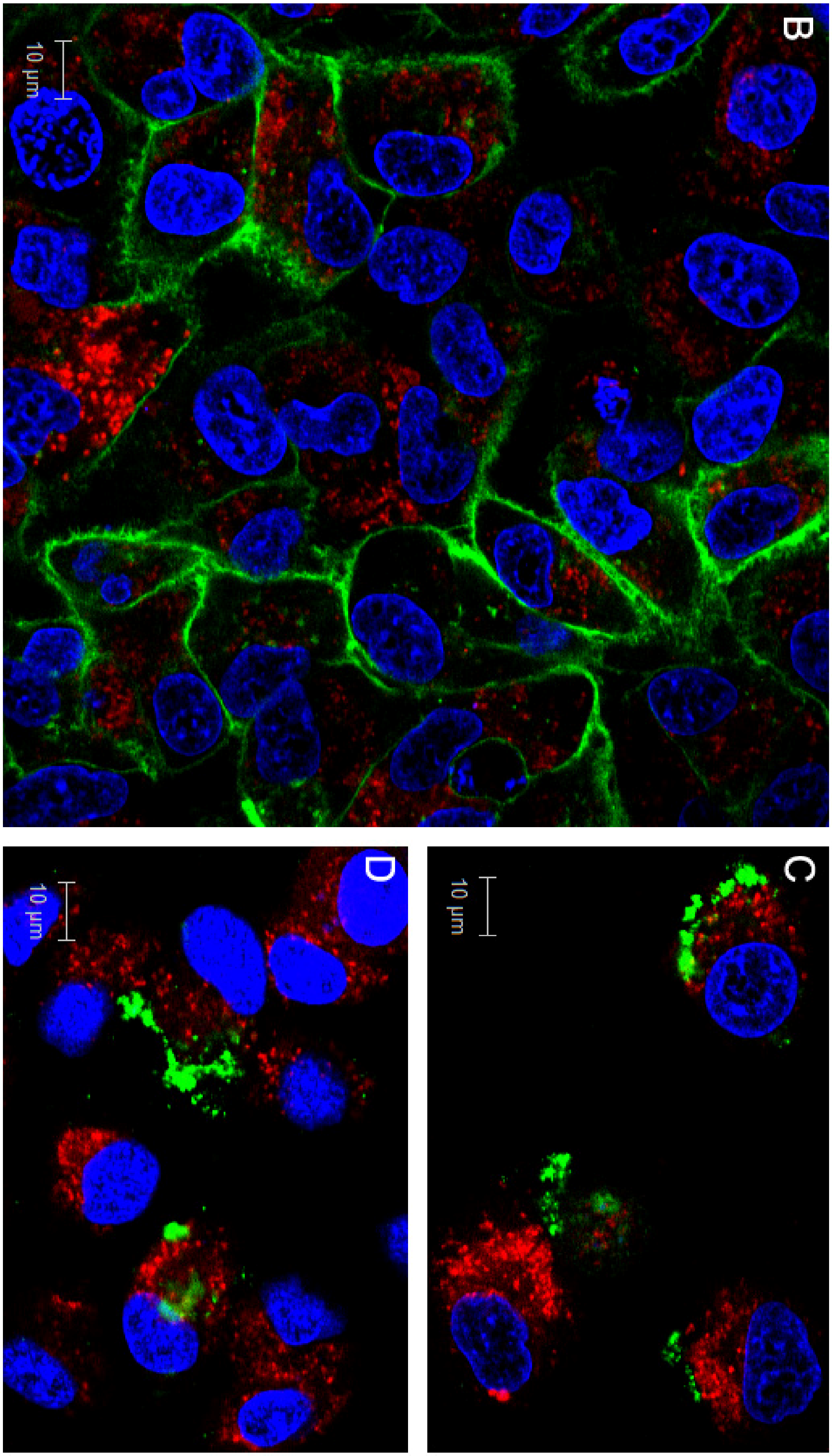
B
10 µm
C
10 µm
D
10 µm

To better examine the location of these puncta on non-permeabilized cells and to further characterize their nature, confocal microscopy was employed to visualize single focal planes of specimens. As shown in Figure 12B-D, staining for HA (green) was abundant at the membranes of most untreated cells. However, cells treated with either CaMe or ActD did not show staining around the periphery of the cell, and instead showed puncta at the cell surface.

3.4 Pharmacological inhibition of CTSB reduces intracellular HA protein in infected cells

Since surface presentation of HA was impaired upon CTSB inhibition, I next investigated the localization of HA within infected cells. The observed lack of HA protein at the cell surface may have been due to problems with protein trafficking. Since CTSB has been shown to have a role in trafficking functions [112, 187], it is plausible that its inhibition may disrupt membrane transport of HA, subsequently targeting cargo for destruction in lysosomes [188-190]. To this end, A549 cells were infected as in Section 3.3, permeabilized, and subsequently stained for both HA (green) and acidified endosomes/lysosomes with the dye LysoTracker (red).

As shown in Figure 13, CaMe-treated cells showed significantly less intracellular staining for HA when compared to untreated cells; ActD-treated cells showed no intracellular staining. Furthermore, there was no apparent colocalization between HA protein and acidified endosomes in any of the conditions (Pearson's coefficients = 0.057, 0.082 and 0.003 for untreated, CaMe-treated and ActD-treated cells, respectively).

3.5 Cholesterol does not accumulate in a CTSB-dependent manner

A growing body of evidence suggests CTSB and other cathepsins are involved in lipid metabolism [161, 162]; recent work has implicated cathepsin D in cholesterol transport from endocytic compartments to the plasma membrane [164, 165]. In the absence of certain cathepsins, including CTSB, lipid metabolism is attenuated, resulting in lipid accumulation in endosomes and/or lysosomes [163]. Many aspects of the influenza lifecycle require a carefully balanced quantity of cholesterol, including entry into host cells [191], progeny

Figure 13 – Inhibition of CTSB in A549 cells with 150 µM CaMe reduces intracellular expression of HA protein.

Coverslips with adherent A549 cells were infected for six hours at a high MOI (5) in the presence of PBS (A), CaMe (150 µM; B), or ActD (5 µg/mL; C). At 5.5 h, LysoTracker Red was added to a final concentration of 200 nM and allowed to incubate for 30 min. At 6 h, coverslips were removed from virus-containing medium and fixed in 4% formaldehyde, permeabilized in 0.25% Triton X-100 for 10 min, and blocked in PBS + 1% BSA + 0.05% Tween 20 for 1 h. Coverslips were then incubated in anti-HA primary antibody at a 1:10 dilution overnight at 4˚C. The following day, slides were washed in PBS and incubated in secondary (anti-mouse FITC) at a 1:100 dilution for 2 h. Slides were then washed once more and incubated in Hoechst 33342 for 3 min at a 1:4000 dilution, rinsed, mounted, and viewed using a Zeiss LSM 510 confocal fluorescence microscope. Images shown are representative cells from respective treatments from three independent experiments, and adjacent images from different z-stack layers (depths). (**A**) Untreated cells showed an abundance of HA (green) as puncta throughout the cell, in the vicinity of acidified endosomes in the cytoplasm (LysoTracker; red). (**B**) Cells treated with CaMe show less puncta inside infected cells. (**C**) ActD-treated cells showed no intracellular puncta, as expected. (**D**) When the number of puncta per cell in at least three random fields of view were quantified, CaMe-treated cells had significantly fewer puncta per cell relative to untreated cells ($p > 0.05$; one-way ANOVA; n=3). Data are expressed as means ± SEM. Columns accompanied by the same letter are not significantly different from each other by Tukey's post hoc test.

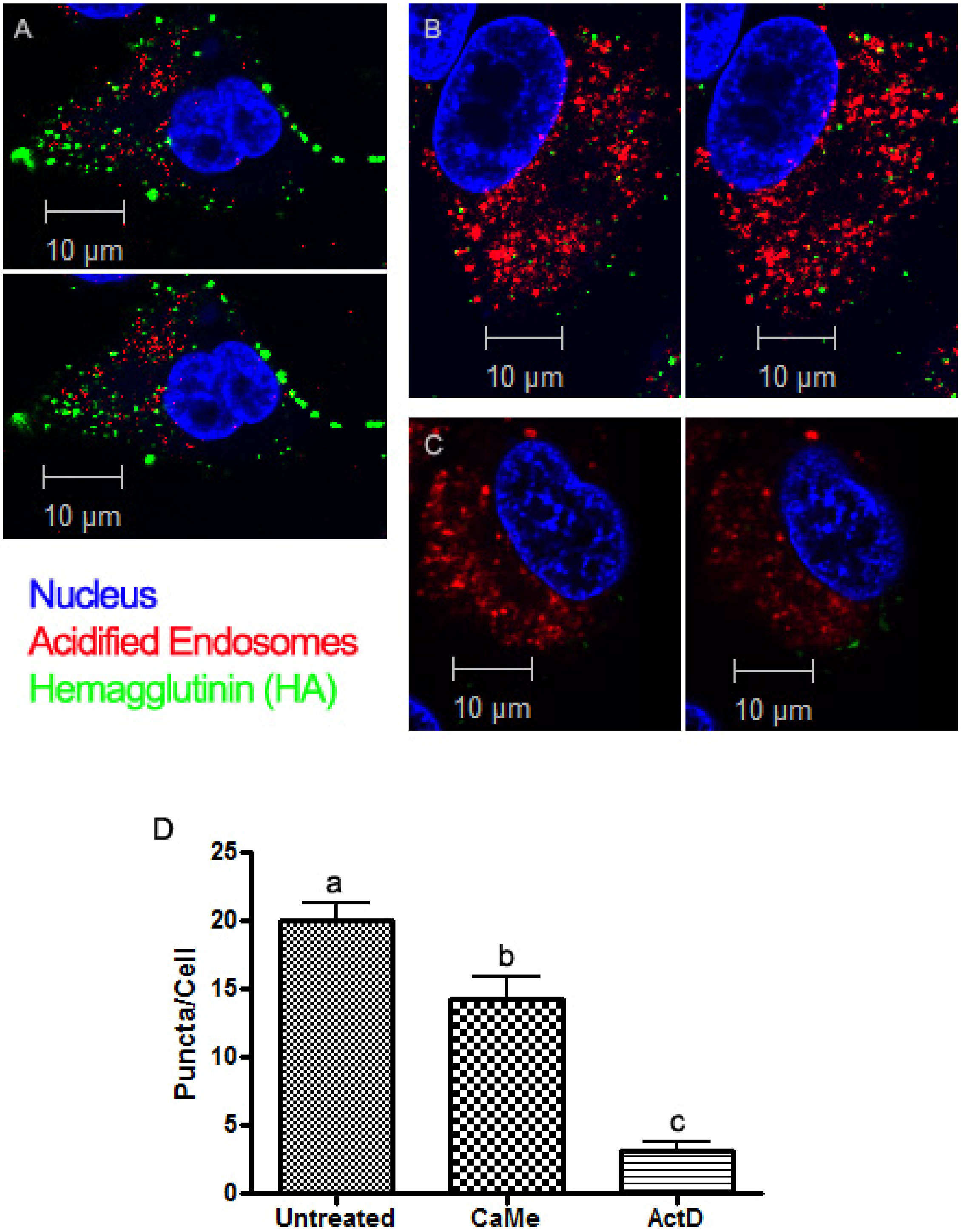
A
10 µm
10 µm
B
10 µm
10 µm
C
10 µm
10 µm
Nucleus
Acidified Endosomes
Hemagglutinin (HA)
D
Puncta/Cell
25
20
15
10
5
0
a
b
c
Untreated
CaMe
ActD

virion assembly and budding [66, 85, 104, 192], the virulence of progeny virus particles [193, 194], and membrane transport of HA [106, 195], neuraminidase [80] and nucleoprotein [196]. Disruptions at any of these stages could result in a marked decrease in viral proliferation. Given the possibility that CTSB is involved in maintaining lipid homeostasis within the cell, it was pertinent to assess whether cholesterol accumulation occurs in its absence, and subsequently whether this was the mechanism responsible for the decreased viral proliferation observed in these cells.

To assess whether a CTSB-deficiency was resulting in the accumulation of cholesterol within endosomes, C57 Wt and KO cells were subjected to sub-cellular fractionation to yield two collections of intracellular components: a crude fraction containing mitochondria, lysosomes, peroxisomes, endoplasmic reticulum and late endosomes; and a purified fraction containing late endosomes and lysosomes. Samples were then assessed for their cholesterol content using the Amplex Red cholesterol assay kit, and values were normalized to those obtained from a Bradford protein assay.

As shown in Figure 14, normalized cholesterol concentrations were not significantly different between Wt and KO cells for either crude organelle or purified endosome/lysosome preparations.

Figure 14 – Endosomal cholesterol accumulation is not responsible for CTSB-dependent influenza A virus restriction.

Wt and KO cells were mechanically homogenized and subjected to differential centrifugation at a low speed (1000 g) to pellet nuclei and cell debris followed by a high speed (20000 g) to pellet organelles (mitochondria, lysosomes, peroxisomes, endoplasmic reticulum, late endosomes; A). Half of this preparation was then further purified by calcium ion precipitation to yield a fraction containing lysosomes and late endosomes (B). Both fractions were then assayed for cholesterol and protein concentration, and cholesterol concentration was normalized to protein content. (**A&B**) When compared to Wt, KO cells showed no significant difference ($p > 0.05$; paired t-test) in the normalized cholesterol concentrations in either organelle (A) or endosomal (B) fractions (n=3). Data are expressed as means ± SEM. N.S. = not significant.

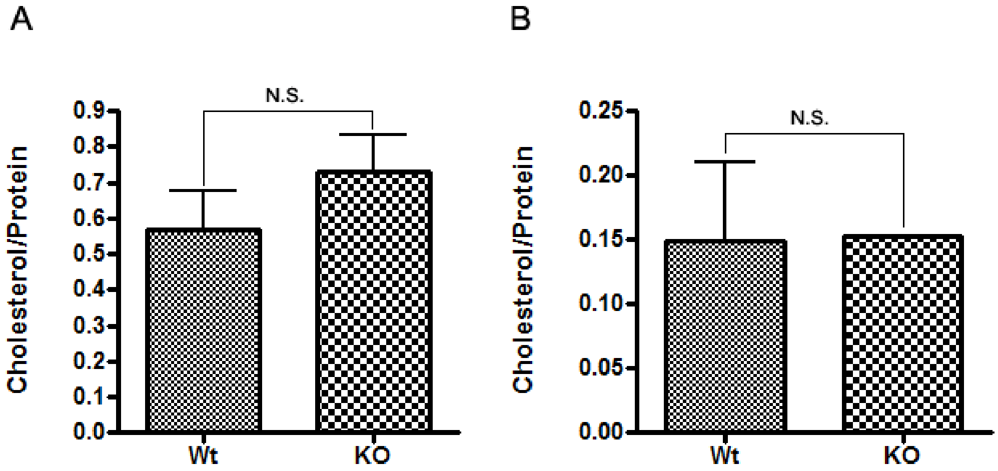
A
B
Cholesterol/Protein
0.9
0.8
0.7
0.6
0.5
0.4
0.3
0.2
0.1
0.0
N.S.
Wt
KO
Cholesterol/Protein
0.25
0.20
0.15
0.10
0.05
0.00
N.S.
Wt
KO

Chapter 4: Discussion

4.1 CTSB is not required for influenza A virus entry or replication

Recent work in our lab identified CTSB as a requirement for HIV release and the propagation of IVA [137]. Cells infected with IVA in the presence of CaMe showed a significant reduction in immunofluorescence compared to untreated cells when stained with pan-specific antibodies against the virus. Work by others indicates CTSB is a requirement in the lifecycles of adeno-associated virus [158], Ebola virus [151, 153, 154], reovirus [136], Nipah virus [156], coronavirus [157], and Moloney murine leukemia virus [138]. In most cases, the role of CTSB is to proteolytically activate viral proteins which facilitate escape into the cytoplasm following endocytosis. Given that CTSB is found mainly in endosomes and IVA uses endosomes to enter host cells, I investigated the role of CTSB in the early stages of the viral lifecycle. Inability of virions to be endocytosed or escape from endosomes could explain the reduction in viral propagation observed previously [137]. To this end, viral load was measured by RT-qPCR in infected cells in the presence or absence of an IVA replication inhibitor, actinomycin D (ActD).

ActD is a transcriptional inhibitor that has been used extensively in influenza research [197-202]. At an appropriate concentration, the drug effectively blocks influenza virus replication (Appendix 1) by preventing nuclear import of the viral genome [198]. Therefore, cells treated with ActD contain only the genetic material and viral proteins endocytosed from the original inoculum, affording an accurate means of assessing viral endocytosis in the absence of replication. RT-qPCR has proven to be a useful tool in quantifying influenza particles [171-173, 203-205]. This is due in part to its sensitivity and the genetic nature of the virus, which packages one copy of each viral gene per virion [179, 180]. Thus, calculations of copy number accurately reflect the absolute number of virions present.

When copy numbers of HA and MA were quantified for infected BMDIM, there were no significant differences between Wt and KO in the copy number of either HA or MA in either the presence or absence of ActD (Figure 4). This data indicates that both Wt and KO cells have similar amounts of viral genetic material after entry (ActD+) and during the early stages of replication (ActD-), suggesting that virion entry into these cells and subsequent replication does not require CTSB.

An identical experiment was performed using the more physiologically relevant A549 lung epithelial cell line and the CTSB inhibitor CaMe at three different concentrations. Similar to findings in the C57 cell line, there were no significant differences in the copy numbers of HA or MA between untreated A549 cells and any of the doses of CaMe both in the presence or absence of ActD (Figure 6).

As expected, cells treated with ActD show a reduction in the copy number of both genes quantified compared to untreated cells, reflecting the drug's ability to inhibit virus replication (Appendix 1). However, one notable difference between the two cell lines used is the titres both achieve. Titres for infected A549 cells in the presence of ActD approach, but never reach 10^5 copies, reflecting approximately 10% of the total number of virus particles used to infect the cells (10^6 for an MOI of 1). Surprisingly, BMDIM under the same conditions routinely reach titres of ~2×10^7 copies, approximately twenty-fold more copies than the inoculum contained. This inconsistency can likely be attributed to the fact that C57 cells are macrophages, and as such will phagocytose pathogens such as influenza virions. When the stock viral inoculum was titred using the above method, it was found that there were approximately 5×10^5 copies of HA and 4×10^5 copies of MA for every titred virion (Appendix 2). Thus, with approximately $4.0 – 5.0 \times 10^{11}$ copies per gene present at an MOI of 1, it is conceivable that a macrophage could engulf ~2.0×10^7 copies. As a result, values for viral entry in BMDIM are likely to be overestimates compared with A549 cells, which are epithelial cells and not phagocytes, and therefore require functional, infectious virions to deliver viral genes to the cell.

The presence of such a large amount of genetic material in the inoculum can be explained by the propensity of influenza virus to generate defective particles in culture [206-208]. The observation of incomplete and non-infectious influenza particles is not a new phenomenon; first documented in the 1950s, it has now become apparent that these structures are produced in the culture of several animal viruses [206, 207]. Indeed, some viruses have been shown to produce several thousand non-infectious particles for every one infectious particle [209]. In the case of influenza, it is believed that the error-prone RNA synthesis of genomes can result in the generation of mutants lacking important genes for replication [210]. Since these mutants have less genetic material, they replicate faster than Wt virus, and can quickly accumulate when propagated in culture. It is likely that the viral inoculum used in this study experienced this fate during its production.

An additional inconsistency between the two cell types is the titre they achieve during active replication. During the six-hour infection period, unabated replication in BMDIM yielded ~7 x 10^7 copies of HA and MA, whereas A549 cells yielded ~3 x 10^8 copies. This may reflect the permissiveness of the respective cell type to infection; evidence suggests that influenza replicates to higher titres in epithelial cells than macrophages [211].

A final variation is evident in the copy numbers of HA and MA from KO cells in the absence of ActD, thereby measuring active replication. Although not statistically significant, the mean copy number of KO MA (3.9 x 10^7 ± 1.4 x 10^7) was nearly half those of KO HA, Wt HA and MA (6.8 x 10^7 – 7.7 x 10^7 ± 2.1 x 10^7). The nature of this discrepancy is unclear; replication in BMDIM as measured by the HA gene showed no such aberration, nor did A549 cells for either gene (Figure 4 & Figure 6). Since this was the only incidence where the copy numbers of HA and MA were not similar, values for this specific treatment should be interpreted with caution.

4.2 A deficiency in CTSB reduces viral HA protein production

After entry and replication, the next logical step to examine is the synthesis of viral proteins. To this end, lysates of infected C57 Wt and KO cells, as well as A549 cells in the presence of different concentrations of CaMe, were separated by SDS-PAGE and probed for viral HA protein by Western blot.

The choice to examine HA over other viral proteins in this and following experiments was twofold. First, HA is absolutely crucial for infectivity [45]; although not obligatory for assembly and release of viral particles [212], virions lacking HA are non-infectious [110] due to an inability to bind host cells or escape endosomes following endocytosis. Second, although HA is not the most abundant protein in virions [185], it is nonetheless produced in modest quantities and composes ~80 % of the protein on virion envelopes [37, 87]. Since the spike glycoprotein is present both inside cells and on the plasma membrane, HA is a pragmatic choice as it affords the ability to assess the outcomes of infection in both compartments.

2.5 hours post-infection, the background of host proteins is dramatically reduced as the machinery is usurped for the production of viral proteins [213-215]. At 3.5 hours post-infection, most viral proteins, including HA, can be easily detected inside infected cells, and have synthesis rates which remain stable up to 10 hours post-infection.

When the concentration of HA protein was examined in cells 6 hours post-infection, strong immunoreactivities were detected in lysates of both C57 (Figure 7) and A549 (Figure 9) cells. The density of these bands was quantified and normalized to those of actin to yield a density for HA which accounted for loading differences between samples. In contrast to entry and replication, C57 KO cells produced significantly less HA protein than Wt cells. This reduction was also evident in infected primary cells of the same genotypes (Figure 8). Likewise, A549 cells treated with 150 µM CaMe produced significantly less HA than untreated cells; a dose dependent reduction in HA protein was evident, but only the 150 µM CaMe treatment reached statistical significance. This reduction was not caused by a decrease in viability as a result of the CaMe treatment (Figure 11).

It is important to note that even the genetic knockout showed some HA protein (Figure 7), suggesting that these cells were, albeit to a lesser extent, still permissive to viral HA production. Thus, it can be concluded that CTSB is required for *optimal* viral HA protein production.

4.3 Pharmacological inhibition of CTSB reduces surface expression of HA protein on infected cells

After synthesis, HA is trafficked via the Golgi to the plasma membrane where it is embedded [87, 103]; budding virions simultaneously acquire both a lipid envelope and anchored HA upon egress from infected cells, thus endowing them with the ability to infect new host cells. Since the amount of HA protein is significantly reduced in CTSB-deficient cells relative to wildtype, it was important to investigate the fate of the HA protein in these cells. It is plausible that differences in the amount of HA protein will impact the amount successfully transported to the cell surface, and therefore onto progeny virions. Since HA is a critical requirement of infection, alterations in the HA protein present on virion envelopes may have important consequences on the virulence of progeny.

To examine the downstream consequences of this reduction in intracellular HA protein, A549 cells were infected in the presence or absence of CaMe, ActD or a combination of the two, and stained for viral HA. Cells were then observed by both immunofluorescence and confocal microscopy to assess the amount of HA on the plasma membrane. A549 cells were selected for these studies because they appeared to yield higher viral titres when compared to C57 cells (Figure 6). Additionally, these cells possess an epithelial morphology, making them larger than macrophages, and therefore facilitate better visualization by microscopy. A single CaMe dose of 150 μM was selected because it yielded a significant reduction in HA protein by Western blot (Figure 9). Finally, since protein synthesis and surface presentation kinetics vary with MOI, a higher MOI was selected for microscopy experiments to not only ensure all cells were infected, but improve the probability of protein expression on the cell surface within a 6 hour infection period [216]. Indeed, fewer cells showed fluorescence for surface HA when infected at an MOI of 1 for 6 hours (data not shown).

When observed using immunofluorescence microscopy, untreated cells showed a diffuse staining pattern for HA across the plasma membrane after infection (Figure 12A); this finding reflects the proper transport of newly synthesized viral HA to the cell surface, where it will be incorporated in the envelopes of budding progeny. However, this staining pattern was not observed in cells treated with ActD (5 μg/mL), CaMe (150 μM) or a combination of the two; instead, only sparse areas of fluorescent puncta were visible on the surface of infected cells.

Since the nature of these puncta remained unclear by immunofluorescence microscopy alone, confocal microscopy was used to examine single focal planes of cells to rule out the possibility that they were simply debris or artefacts in the preparation, rather than the cells themselves. When specimens were prepared and observed using confocal microscopy, a similar staining pattern was observed (Figure 12B-D). As expected, untreated cells showed abundant staining for HA protein across the plasma membrane upon infection with IVA. Interestingly, similar to Figure 12A, CaMe- and ActD-treated cells showed no diffuse staining across the periphery of the cell, but puncta in limited areas of the membrane. It is important to note that these puncta are observable in the same focal plane as intracellular organelles (lysosomes, red; nucleus, blue), but adjacent to the cells themselves.

The absence of HA on the membranes of ActD-treated cells conforms to expectations; since no HA protein is produced in this treatment (Appendix 1), logic dictates that no protein will be presented on the surface of these infected cells. Strikingly, CaMe-treated cells showed a very similar phenotype, suggesting that they too failed to present HA on the cell surface. However, unlike ActD-treated cells, HA was indeed present in CaMe-treated cells, albeit at lower concentrations than in untreated controls (Figure 9).

The puncta on the surface of CaMe- and ActD-treated cells are not likely the result of viral activity. Since ActD treatment abolished both replication (Figure 6) and HA protein production (Appendix 1), it is doubtful these puncta represent HA originating from within infected cells. As similar puncta were observed in CaMe-treated cells, it is conceivable that these too resulted from a phenomenon external to infection. This notion is supported by the presence of similar puncta in control conditions which lack primary (anti-HA) antibody (Appendix 3), suggesting they may be the product of non-specific binding of the secondary antibody. Additionally, it is also possible that large numbers of defective particles in the inoculum aggregated at the cell surface, where they were subsequently fixed and stained.

Nonetheless, it is clear that CaMe-treatment impaired the surface presentation of HA protein. Collectively, these data suggest that in addition to optimal HA protein production, CTSB is also a requisite for proper presentation of HA on the surface of infected cells. However, this observation fails to explain the apparent discrepancy between the levels of intracellular HA protein and that presented on the surface of CaMe-treated infected cells. Were HA presentation a mere function of the intracellular concentration of the protein, a reduction in intracellular HA would be expected to reduce surface expression of the protein in a proportional manner. However, these data show a complete absence of observable HA on the surface of CaMe-treated infected cells in spite of having detectable levels of HA protein (Figure 9). This suggests that an additional CTSB-dependent mechanism is involved in the successful translocation of HA protein to the surface of infected cells.

4.4 Pharmacological inhibition of CTSB reduces intracellular HA protein in infected cells

While the effects of CTSB-inhibition on intracellular (Figure 9) and membrane-associated (Figure 12) HA protein were apparent, the cause of these reductions remained elusive. Indeed, several possible explanations exist, thus necessitating a more detailed examination into the location of HA within CaMe-treated infected cells.

Although CTSB is commonly known for its proteolytic functions, paradoxically, the reduction in HA protein may be caused by its absence. Recent research suggests that in addition to classically defined roles, CTSB is also involved in the trafficking of proteins [187] and vesicles [112]. The latter is of particular interest, as the transport of HA is analogous to that of TNF-α, the subject of prior research. HA, like TNF-α, is transported through the Golgi to the cell surface [87, 217]. In the absence of functional CTSB, TNF-α failed to reach the plasma membrane, and instead accumulated in intracellular vesicles [112]. Likewise, inhibition of CTSB resulted in a failure to release HIV-1 virus-like particles, instead retaining them within host cell compartments [137]. Thus, since HA failed to reach the membranes of CaMe-treated cells, it is possible that HA protein may be transported through a similar CTSB-dependent mechanism.

However, intracellular HA protein was reduced in CTSB-deficient cells (Figure 7; Figure 9), making it unlikely that HA was accumulating inside vesicles as was the case for TNF-α. One mechanism by which intracellular protein levels can be depleted involves lysosomal degradation. Lysosomes are acidic organelles which contain a variety of enzymes used to digest proteins and other macromolecular structures in the cell [218]. In the context of the IVA lifecycle, a possible scenario in which CTSB-dependent HA transport is impaired may result in the inadvertent delivery of HA proteins to lysosomes, where they are subsequently degraded [188-190]. Instances where proteins or vesicles are improperly targeted to lysosomes due to defects in their respective transport systems have been noted in literature previously [219-221].

Since the above scenario could potentially explain both the decrease in intracellular HA protein and its absence on the surface of CaMe-treated infected cells, the localization of intracellular HA was assessed using confocal microscopy, particularly in regard to lysosomes. To this end, A549 cells were infected in the presence or absence of CaMe and ActD in the same manner as cells prepared for Section 3.3 with the addition of a permeabilization step to allow for immunostaining of HA within cells. Lysosomes were visualized using LysoTracker, a membrane-permeable fluorophore that preferentially accumulates in acidic organelles such as lysosomes or acidified late endosomes [222].

When CaMe-treated cells were examined, both the number and size of intracellular HA puncta were noticeably reduced when compared to untreated cells (Figure 13). As expected, ActD-treated cells showed no intracellular puncta. These observations were all in agreement with immunoblot analyses for HA (Figure 9; Appendix 1). However, there was no visible colocalization between HA protein (green) and lysosomes (red) in any of the conditions, which would have been indicative by a yellow colour. Fluorescence colocalization can also be mathematically quantified by means of a Pearson's coefficient, which expresses the degree of overlap between two fluorescence channels in terms of a numeric value [223]. Since a value of 0 represents a complete lack of correlation, respective Pearson's coefficients of 0.057, 0.082 and 0.003 for untreated, CaMe-treated, and ActD-treated cells also support visual observations.

It is worth noting that LysoTracker has been reported to undergo photoconversion under certain conditions [224]. The resulting green fluorescence emitted can overlap with other dyes at this wavelength such as FITC, which was used in labelling for HA. However, since there was both minimal colocalization of these channels in all treatments, and no observable green fluorescence detected in most ActD-treated cells (Figure 13), it is highly unlikely this effect took place in this study. As such, it is doubtful that puncta indicative of HA can be attributed to LysoTracker. Additionally, there was also a noticeable reduction in membrane puncta between permeabilized and unpermeabilized cells (compare Figure 13C with Figure 12D). This can likely be attributed to the permeabilization procedure, which causes significant damage to the membrane, thereby increasing the chances of non-specific binding at the cell surface being removed.

Collectively, these data do not substantiate the notion that lysosomal degradation is the cause of HA protein reduction within, and absence on the surface of CTSB-deficient cells. An alternative pathway of protein degradation – the proteosome – was also investigated as the cause of CTSB-dependent decreases in intracellular HA. However, preliminary studies using the proteosome inhibitor MG132 did not appear to result in visible increases of HA protein in C57 KO cells (data not shown). Since MG132-treatment is not a comprehensive means of inhibiting all protein degradation pathways, degradation of HA protein in CTSB-deficient cells remains a possibility. Thus, an alternate mechanism is the source of intracellular HA protein reduction and/or unsuccessful transport to the plasma membrane of CaMe-treated infected cells.

4.5 Cholesterol does not accumulate in a CTSB-dependent manner

Since lysosomal intervention was uninvolved in the fate of HA protein in CTSB-deficient cells, a new mechanism was sought to explain the differences in HA expression between cells with and without functional CTSB. A more exotic postulate for this phenomenon may involve transport systems for lipids such as cholesterol.

Recent work implicates CTSB and other members of the cathepsin family are involved in the metabolism of lipids [161, 162]; for example, cathepsin D has been implicated in cholesterol transport from endocytic compartments to the plasma membrane [164, 165]. Importantly, the absence of certain cathepsins, such as CTSB, results in the attenuation of lipid metabolism and accumulation of lipids in endocytic vesicles and/or lysosomes [163]. A functionally homologous condition can be found in cells bearing mutations in the gene *NPC1*, resulting in Niemann-Pick disease, type C. NPC1 is an intracellular cholesterol transporter; loss of function results in a dramatic accumulation of lipids in late endosomes and lysosomes and aberrant trafficking of these vesicles [165-169].

Interestingly, human immunodeficiency virus (HIV) release is impaired in NPC1$^{-/-}$ cells [225]; this was accompanied by a concomitant trapping of the viral structural protein, Gag, inside endosomes and lysosomes [226]. Another enveloped virus, Ebola virus, showed an inability to infect NPC1$^{-/-}$ cells due to a failure in escaping from endosomes following entry into host cells [227, 228].

Cholesterol is a lipid sterol that is essential for the maintenance of membrane dynamics, fluidity and permeability, among other functions [229]. Given that IVA is an enveloped virus, is it perhaps not surprising that it also shares a similar dependence on cholesterol levels which are adequate, but not excessive.

Indeed, several facets in the influenza lifecycle can be affected by changes in cholesterol. Cholesterol is critical for IVA virion entry; depletion of viral envelopes significantly reduces virion infectivity, possibly by disrupting the fusion process [191]. Additionally, cholesterol is a major constituent of lipid rafts, microdomains in the plasma membrane which serve as sites for virion assembly and budding [85, 104, 108, 192]. As such, multiple viral proteins are targeted here, including nucleoprotein cores [196] and spike glycoproteins neuraminidase [80] and HA [106, 195]. It is postulated that lipid rafts facilitate the concentration of viral proteins in order to reach sufficient concentrations for assembly and budding; in the case of HA, it is thought that this strategy ensures adequate protein will be present on the envelopes of budding progeny to effectively mediate membrane fusion with a new host cell [66].

Disrupting lipid rafts by cholesterol depletion reportedly enhanced the release of viral particles, but these particles displayed reduced infectivity [193]. The authors proposed this was the result of multiple consequences associated with cholesterol reduction, such as altered structural integrity of virions or the stability of their membranes. Interestingly, the interferon-inducible antiviral protein viperin inhibits the release of IVA virions by disrupting lipid rafts [230]. Finally, the use of cholesterol-reducing drugs *in vivo* has also been linked to a decrease in mortality as a result of influenza infection, though the observational study did not propose a mechanism for this [231, 232].

Considering that obstructions to any of the above processes may result in a marked decrease in viral proliferation, including problems targeting HA to the membrane, it was pertinent to investigate whether observations in CTSB-deficient cells are a consequence of cholesterol dysregulation. The endosomal accumulation of lipids like cholesterol may not only result in improper trafficking of vesicles containing viral components, but may also reflect an impairment of cholesterol transport to the membrane, thus affecting lipid rafts as well.

To assess the role of CTSB in the accumulation of cholesterol within endosomes, C57 Wt and KO cells were fractionated to yield subcellular organelles, and both cholesterol and protein contents were quantified using Amplex Red and Bradford assays, respectively.

When Wt and KO cells were compared, normalized cholesterol concentrations were not significantly different for either the crude or purified preparations (Figure 14). The finding that cholesterol is similar in both fractions between these cell types indicates cholesterol does not accumulate in a CTSB-dependent manner, and consequently is unlikely to be the mechanism behind IVA restriction in these cells. However, it should be noted that since this assay examined the cholesterol of intracellular organelles, it does not preclude the possibility of CTSB-dependent alterations to lipid rafts in the plasma membrane.

4.6 Future directions

At present, the role CTSB plays in the influenza lifecycle remains unclear. When viral titres were assessed using a hemagglutination assay, there were no significant differences between the supernatants of A549 cells infected for 24 hours in the presence or absence of 150 µM CaMe (Appendix 4). It is worth noting that a hemagglutination assay measures viral titres on the basis of HA protein on the surface of particles, and consequently is unable to distinguish between infectious and defective particles. Thus, although particles appear to be released from infected cells in the presence of CaMe, and interestingly, bear comparable amounts of HA protein as those released from untreated cells, whether these particles are functional could not be definitively ascertained. It is possible that a CTSB-deficiency delays the surface expression of HA, and that the longer incubation period used in the hemagglutination assay affords more time for its incorporation into the host membrane and subsequently budding virions [216]. Additionally, it would be of interest to determine whether these observations are unique to HA or apply to other viral proteins whose synthesis and trafficking are both similar (NA) and dissimilar (nucleoprotein) to HA.

It was recently reported that influenza infection elevates CTSB in murine cells [233], which, in agreement with this work, suggests that it plays an important role in the viral lifecycle. However, the reduced intracellular, but absent surface expression of HA in CTSB-deficient cells remains an unresolved discrepancy. Proposed mechanisms involving lysosomal degradation and cholesterol accumulation could not be substantiated as the cause of these phenomena.

It is possible that both observations could result from separate yet related processes involving a requirement for CTSB. The reduction in intracellular HA could not be definitively attributed to post-translational degradation, nor could differences in protein synthesis be ruled out. It is possible that cathepsins like CTSB function as transcriptional activators for viral genes such as HA [234, 235]. This could perhaps explain why a CTSB-deficiency *attenuated* HA protein levels, rather than abolish them entirely.

Alternatively, the role of CTSB may be independent from facilitating the production and transport of HA to the infected cell membrane, with these observations being mere consequences of a different pathway. For example, influenza has been shown to require the process of autophagy for optimal replication for reasons not fully understood at this time, but possibly involving cell death [183, 236-242]. CTSB is increasingly being connected with autophagy, including cell death responses [118, 187, 243-245]. Similarly, it has been shown the virus activates the host inflammatory response [246], possibly due to a reliance on caspase 3 for nuclear exit of ribonucleoprotein cores [247, 248]. If the virus relies on inflammasome activation to make use of caspase 3, it is of interest that CTSB has been reported to be involved in inflammasome activation [113, 114], the stimulation of caspase 3 [249], and the catalytic activation of Toll-like receptor 3 [250], which IVA uses to stimulate the inflammasome. Thus, there are many potential avenues in the search for mechanistic details of CTSB-dependent influenza virus restriction.

Resistance of circulating IVA strains to older antivirals such as amantadine has increased at an alarming rate over the past decade [251]; as a result, the CDC no longer recommends the use of these drugs in the treatment of influenza infections [252]. Resistance to newer antivirals such as oseltamivir (Tamiflu®) has also been documented, in spite of earlier reports which erroneously suggested such resistance-conferring mutations would significantly compromise viral fitness as a result, making them an unlikely threat [253, 254]. Given the rate with which antiviral therapies are becoming obsolete due to viral mutations, a more effective strategy would be to target host rather than viral components required for the effective replication of IVA. CTSB is an essential human protease which serves a number of important functions within healthy cells; as such, it is not feasible to treat IVA infections with a CTSB-inhibitor like CaMe. However, future work should endeavour to further delineate the role of CTSB as a requirement for IVA infection and/or propagation. Greater knowledge of the host systems the virus exploits within infected cells may shed light on new targets for antiviral therapies less prone to resistance.

Chapter 5: References

1. WHO. *Seasonal Influenza Factsheet*. 2009 April 10/13]; Available from: http://www.who.int/mediacentre/factsheets/fs211/en/index.html.
2. WHO. *Avian Influenza Factsheet*. 2011 April 10/13]; Available from: http://www.who.int/mediacentre/factsheets/avian_influenza/en/.
3. Rothberg, M.B., S.D. Haessler, and R.B. Brown, *Complications of viral influenza.* Am J Med, 2008. **121**(4): p. 258-264.
4. Metersky, M.L., et al., *Epidemiology, microbiology, and treatment considerations for bacterial pneumonia complicating influenza.* Int J Infect Dis, 2012. **16**(5): p. E321-E331.
5. Klenk, *Avian Influenza: Molecular Mechanisms of Pathogenesis and Host Range*, in *Animal Viruses: Molecular Biology*, C.A. Press, Editor. 2008.
6. Osterhaus, A.D.M.E., et al., *Influenza B virus in seals.* Science, 2000. **288**(5468): p. 1051-1053.
7. Matsuzaki, Y., et al., *Clinical features of influenza C virus infection in children.* J Infect Dis, 2006. **193**(9): p. 1229-1235.
8. CDC. *Influenza Activity - The United States - 2011/2012*. 2012 April 10/13]; Available from: http://www.cdc.gov/mmwr/preview/mmwrhtml/mm6122a4.htm.
9. Matsuzaki, Y., et al., *Antigenic and genetic characterization of influenza C viruses which caused two outbreaks in Yamagata City, Japan, in 1996 and 1998.* J Clin Microbiol, 2002. **40**(2): p. 422-429.
10. Palese, P., Shaw, M.L, *Orthomyxoviridae: the viruses and their replication*. Fields Virology, ed. D.M. Knipe, Howley, P.M. 2007, Philadelphia: Lippincott Williams & Wilkins.
11. Rossman, J.S. and R.A. Lamb, *Influenza virus assembly and budding.* Virology, 2011. **411**(2): p. 229-36.
12. Liu, C., et al., *Influenza type A virus neuraminidase does not play a role in viral entry, replication, assembly, or budding.* J Virol, 1995. **69**(2): p. 1099-106.
13. Lamb, R.A., S.L. Zebedee, and C.D. Richardson, *Influenza virus M2 protein is an integral membrane protein expressed on the infected-cell surface.* Cell, 1985. **40**(3): p. 627-33.
14. Iwatsuki-Horimoto, K., et al., *The cytoplasmic tail of the influenza A virus M2 protein plays a role in viral assembly.* J Virol, 2006. **80**(11): p. 5233-40.
15. Rossman, J.S., et al., *Influenza virus M2 protein mediates ESCRT-independent membrane scission.* Cell, 2010. **142**(6): p. 902-13.
16. Chen, B.J., et al., *The influenza virus M2 protein cytoplasmic tail interacts with the M1 protein and influences virus assembly at the site of virus budding.* J Virol, 2008. **82**(20): p. 10059-70.
17. Ye, Z., et al., *Association of influenza virus matrix protein with ribonucleoproteins.* J Virol, 1999. **73**(9): p. 7467-73.
18. Ali, A., et al., *Influenza virus assembly: effect of influenza virus glycoproteins on the membrane association of M1 protein.* J Virol, 2000. **74**(18): p. 8709-19.
19. Elton, D., et al., *Identification of amino acid residues of influenza virus nucleoprotein essential for RNA binding.* J Virol, 1999. **73**(9): p. 7357-67.

20. Portela, A. and P. Digard, *The influenza virus nucleoprotein: a multifunctional RNA-binding protein pivotal to virus replication.* J Gen Virol, 2002. **83**(Pt 4): p. 723-34.
21. Toyoda, T., et al., *Molecular assembly of the influenza virus RNA polymerase: determination of the subunit-subunit contact sites.* J Gen Virol, 1996. **77 (Pt 9)**: p. 2149-57.
22. Poole, E., et al., *Functional domains of the influenza A virus PB2 protein: identification of NP- and PB1-binding sites.* Virology, 2004. **321**(1): p. 120-33.
23. Guo, Z., et al., *NS1 protein of influenza A virus inhibits the function of intracytoplasmic pathogen sensor, RIG-I.* Am J Respir Cell Mol Biol, 2007. **36**(3): p. 263-9.
24. Gack, M.U., et al., *Influenza A virus NS1 targets the ubiquitin ligase TRIM25 to evade recognition by the host viral RNA sensor RIG-I.* Cell Host Microbe, 2009. **5**(5): p. 439-49.
25. Jia, D., et al., *Influenza virus non-structural protein 1 (NS1) disrupts interferon signaling.* PLoS One, 2010. **5**(11): p. e13927.
26. Paterson, D. and E. Fodor, *Emerging roles for the influenza A virus nuclear export protein (NEP).* PLoS Pathog, 2012. **8**(12): p. e1003019.
27. Chen, W.S., et al., *A novel influenza A virus mitochondrial protein that induces cell death.* Nat Med, 2001. **7**(12): p. 1306-1312.
28. Gibbs, J.S., et al., *The influenza A virus PB1-F2 protein targets the inner mitochondrial membrane via a predicted basic amphipathic helix that disrupts mitochondrial function.* J Virol, 2003. **77**(13): p. 7214-24.
29. Fujiyoshi, Y., et al., *Fine structure of influenza A virus observed by electron cryo-microscopy.* EMBO J, 1994. **13**(2): p. 318-26.
30. Morgan, C., H.M. Rose, and D.H. Moore, *Structure and development of viruses observed in the electron microscope. III. Influenza virus.* J Exp Med, 1956. **104**(2): p. 171-82.
31. Noda, T., et al., *Architecture of ribonucleoprotein complexes in influenza A virus particles.* Nature, 2006. **439**(7075): p. 490-2.
32. Roberts, P.C., R.A. Lamb, and R.W. Compans, *The M1 and M2 proteins of influenza A virus are important determinants in filamentous particle formation.* Virology, 1998. **240**(1): p. 127-37.
33. CDC. *Influenza Viruses*. 2005 April 10/13]; Available from: http://www.cdc.gov/flu/avian/gen-info/flu-viruses.htm.
34. Nobusawa, E. and K. Sato, *Comparison of the mutation rates of human influenza A and B viruses.* J Virol, 2006. **80**(7): p. 3675-8.
35. Ndifon, W., N.S. Wingreen, and S.A. Levin, *Differential neutralization efficiency of hemagglutinin epitopes, antibody interference, and the design of influenza vaccines.* Proc Natl Acad Sci U S A, 2009. **106**(21): p. 8701-8706.
36. Garten, R.J., et al., *Antigenic and Genetic Characteristics of Swine-Origin 2009 A(H1N1) Influenza Viruses Circulating in Humans.* Science, 2009. **325**(5937): p. 197-201.
37. Lamb, R.A., Krug, R.M., *Orthomyxoviridae: the viruses and their replication.* Fundamental Virology, ed. L.W. Wilkins. 2001, Philadelphia, PA.
38. Pan, C.E., et al., *Genomic Signature and Mutation Trend Analysis of Pandemic (H1N1) 2009 Influenza A Virus.* PLoS One, 2010. **5**(3): p. A31-A37.

39. Zambon, M.C., *Epidemiology and pathogenesis of influenza.* Journal of Antimicrobial Chemotherapy, 1999. **44**: p. 3-9.
40. Bautista, E., et al., *Medical Progress: Clinical Aspects of Pandemic 2009 Influenza A (H1N1) Virus Infection.* New England Journal of Medicine, 2010. **362**(18): p. 1708-1719.
41. Matlin, K.S., et al., *Infectious entry pathway of influenza virus in a canine kidney cell line.* J Cell Biol, 1981. **91**(3 Pt 1): p. 601-13.
42. Kumlin, U., et al., *Sialic acid tissue distribution and influenza virus tropism.* Influenza Other Respi Viruses, 2008. **2**(5): p. 147-54.
43. Shinya, K., et al., *Avian flu: influenza virus receptors in the human airway.* Nature, 2006. **440**(7083): p. 435-6.
44. Thompson, C.I., et al., *Infection of human airway epithelium by human and avian strains of influenza a virus.* J Virol, 2006. **80**(16): p. 8060-8.
45. Jiang, S., et al., *Roles of the hemagglutinin of influenza A virus in viral entry and development of antiviral therapeutics and vaccines.* Protein Cell, 2010. **1**(4): p. 342-54.
46. Rust, M.J., et al., *Assembly of endocytic machinery around individual influenza viruses during viral entry.* Nat Struct Mol Biol, 2004. **11**(6): p. 567-73.
47. Luo, M., *Influenza Virus Entry.* Advances in Experimental Medicine and Biology, ed. M.G.a.R. Rossmann, V.B. . Vol. 726. 2012.
48. Lakadamyali, M., et al., *Visualizing infection of individual influenza viruses.* Proc Natl Acad Sci U S A, 2003. **100**(16): p. 9280-9285.
49. Cross, K.J., L.M. Burleigh, and D.A. Steinhauer, *Mechanisms of cell entry by influenza virus.* Expert Rev Mol Med, 2001. **3**(21): p. 1-18.
50. Helenius, A., *Unpacking the Incoming Influenza-Virus.* Cell, 1992. **69**(4): p. 577-578.
51. Pinto, L.H., L.J. Holsinger, and R.A. Lamb, *Influenza virus M2 protein has ion channel activity.* Cell, 1992. **69**(3): p. 517-28.
52. Martin, K. and A. Helenius, *Transport of incoming influenza virus nucleocapsids into the nucleus.* J Virol, 1991. **65**(1): p. 232-44.
53. Deng, T., F.T. Vreede, and G.G. Brownlee, *Different de novo initiation strategies are used by influenza virus RNA polymerase on its cRNA and viral RNA promoters during viral RNA replication.* J Virol, 2006. **80**(5): p. 2337-2348.
54. Nagata, K., A. Kawaguchi, and T. Naito, *Host factors for replication and transcription of the influenza virus genome.* Rev Med Virol, 2008. **18**(4): p. 247-60.
55. Dhar, R., R.M. Chanock, and C.J. Lai, *Non-Viral Oligonucleotides at the 5' Terminus of Cytoplasmic Influenza Viral Messenger-Rna Deduced from Cloned Complete Genomic Sequences.* Cell, 1980. **21**(2): p. 495-500.
56. Engelhardt, O.G., M. Smith, and E. Fodor, *Association of the influenza a virus RNA-dependent RNA polymerase with cellular RNA polymerase II.* J Virol, 2005. **79**(9): p. 5812-5818.
57. Garfinkel, M.S. and M.G. Katze, *Translational control by influenza virus. Selective translation is mediated by sequences within the viral mRNA 5'-untranslated region.* J Biol Chem, 1993. **268**(30): p. 22223-6.
58. Katze, M.G. and R.M. Krug, *Metabolism and expression of RNA polymerase II transcripts in influenza virus-infected cells.* Mol Cell Biol, 1984. **4**(10): p. 2198-206.

59. Katze, M.G., Y.T. Chen, and R.M. Krug, *Nuclear-cytoplasmic transport and VAI RNA-independent translation of influenza viral messenger RNAs in late adenovirus-infected cells.* Cell, 1984. **37**(2): p. 483-90.
60. Katze, M.G., D. DeCorato, and R.M. Krug, *Cellular mRNA translation is blocked at both initiation and elongation after infection by influenza virus or adenovirus.* J Virol, 1986. **60**(3): p. 1027-39.
61. Garfinkel, M.S. and M.G. Katze, *Translational Control by Influenza-Virus - Selective and Cap-Dependent Translation of Viral Messenger-Rnas in Infected-Cells.* J Biol Chem, 1992. **267**(13): p. 9383-9390.
62. Park, Y.W., J. Wilusz, and M.G. Katze, *Regulation of eukaryotic protein synthesis: selective influenza viral mRNA translation is mediated by the cellular RNA-binding protein GRSF-1.* Proc Natl Acad Sci U S A, 1999. **96**(12): p. 6694-9.
63. Katze, M.G., et al., *Translational control by influenza virus: suppression of the kinase that phosphorylates the alpha subunit of initiation factor eIF-2 and selective translation of influenza viral mRNAs.* Mol Cell Biol, 1986. **6**(5): p. 1741-50.
64. Das, K., et al., *Structures of influenza A proteins and insights into antiviral drug targets.* Nat Struct Mol Biol, 2010. **17**(5): p. 530-538.
65. Leser, G.P. and R.A. Lamb, *Influenza virus assembly and budding in raft-derived microdomains: a quantitative analysis of the surface distribution of HA, NA and M2 proteins.* Virology, 2005. **342**(2): p. 215-27.
66. Takeda, M., et al., *Influenza virus hemagglutinin concentrates in lipid raft microdomains for efficient viral fusion.* Proc Natl Acad Sci U S A, 2003. **100**(25): p. 14610-7.
67. Marjuki, H., et al., *Membrane accumulation of influenza A virus hemagglutinin triggers nuclear export of the viral genome via protein kinase Calpha-mediated activation of ERK signaling.* J Biol Chem, 2006. **281**(24): p. 16707-15.
68. Baudin, F., et al., *In vitro dissection of the membrane and RNP binding activities of influenza virus M1 protein.* Virology, 2001. **281**(1): p. 102-8.
69. Boulo, S., et al., *Nuclear traffic of influenza virus proteins and ribonucleoprotein complexes.* Virus Res, 2007. **124**(1-2): p. 12-21.
70. Neumann, G., M.T. Hughes, and Y. Kawaoka, *Influenza A virus NS2 protein mediates vRNP nuclear export through NES-independent interaction with hCRM1.* EMBO J, 2000. **19**(24): p. 6751-8.
71. Akarsu, H., et al., *Crystal structure of the M1 protein-binding domain of the influenza A virus nuclear export protein (NEP/NS2).* EMBO J, 2003. **22**(18): p. 4646-55.
72. Martin, K. and A. Helenius, *Nuclear transport of influenza virus ribonucleoproteins: the viral matrix protein (M1) promotes export and inhibits import.* Cell, 1991. **67**(1): p. 117-30.
73. Jo, S., et al., *Involvement of vesicular trafficking system in membrane targeting of the progeny influenza virus genome.* Microbes Infect, 2010. **12**(12-13): p. 1079-84.
74. Eisfeld, A.J., et al., *RAB11A Is Essential for Transport of the Influenza Virus Genome to the Plasma Membrane.* J Virol, 2011. **85**(13): p. 6117-6126.
75. Momose, F., et al., *Apical transport of influenza A virus ribonucleoprotein requires Rab11-positive recycling endosome.* PLoS One, 2011. **6**(6): p. e21123.
76. Fujii, Y., et al., *Selective incorporation of influenza virus RNA segments into virions.* Proceedings of the Proc Natl Acad Sci U S A, 2003. **100**(4): p. 2002-2007.

77. Muramoto, Y., et al., *Hierarchy among viral RNA (vRNA) segments in their role in vRNA incorporation into influenza A virions.* J Virol, 2006. **80**(5): p. 2318-2325.
78. Chen, B.J., et al., *Influenza virus hemagglutinin and neuraminidase, but not the matrix protein, are required for assembly and budding of plasmid-derived virus-like particles.* J Virol, 2007. **81**(13): p. 7111-23.
79. Ali, A., et al., *Influenza virus assembly: Effect of influenza virus glycoproteins on the membrane association of M1 protein.* J Virol, 2000. **74**(18): p. 8709-8719.
80. Barman, S., et al., *Role of transmembrane domain and cytoplasmic tail amino acid sequences of influenza a virus neuraminidase in raft association and virus budding.* J Virol, 2004. **78**(10): p. 5258-69.
81. Noton, S.L., et al., *Identification of the domains of the influenza A virus M1 matrix protein required for NP binding, oligomerization and incorporation into virions.* J Gen Virol, 2007. **88**(Pt 8): p. 2280-90.
82. Watanabe, R. and R.A. Lamb, *Influenza virus budding does not require a functional AAA+ ATPase, VPS4.* Virus Res, 2010. **153**(1): p. 58-63.
83. Bruce, E.A., et al., *Budding of filamentous and non-filamentous influenza A virus occurs via a VPS4 and VPS28-independent pathway.* Virology, 2009. **390**(2): p. 268-78.
84. Yondola, M. and C. Carter, *Un-"ESCRT"-ed budding.* Viruses, 2011. **3**(1): p. 26-31.
85. Schroeder, C., et al., *The influenza virus ion channel and maturation cofactor M2 is a cholesterol-binding protein.* Eur Biophys J, 2005. **34**(1): p. 52-66.
86. Palese, P., et al., *Characterization of temperature sensitive influenza virus mutants defective in neuraminidase.* Virology, 1974. **61**(2): p. 397-410.
87. Nayak, D.P., E.K. Hui, and S. Barman, *Assembly and budding of influenza virus.* Virus Res, 2004. **106**(2): p. 147-65.
88. Hirst, G.K., *The Agglutination of Red Cells by Allantoic Fluid of Chick Embryos Infected with Influenza Virus.* Science, 1941. **94**(2427): p. 22-3.
89. Nicholls, J.M., Lai, J., Garcia, J.M., *Investigating the Interaction Between Influenza and Sialic Acid: Making and Breaking the Link*, in *Influenza Virus Sialidase - A Drug Discovery Target*, M. von Itzstein, Editor. 2012, Springer Basel. p. 31-45.
90. Weis, W., et al., *Structure of the influenza virus haemagglutinin complexed with its receptor, sialic acid.* Nature, 1988. **333**(6172): p. 426-31.
91. Eisen, M.B., et al., *Binding of the influenza A virus to cell-surface receptors: structures of five hemagglutinin-sialyloligosaccharide complexes determined by X-ray crystallography.* Virology, 1997. **232**(1): p. 19-31.
92. Sauter, N.K., et al., *Hemagglutinins from two influenza virus variants bind to sialic acid derivatives with millimolar dissociation constants: a 500-MHz proton nuclear magnetic resonance study.* Biochemistry, 1989. **28**(21): p. 8388-96.
93. Hanson, J.E., et al., *Proton nuclear magnetic resonance studies of the binding of sialosides to intact influenza virus.* Virology, 1992. **189**(2): p. 525-33.
94. Takemoto, D.K., J.J. Skehel, and D.C. Wiley, *A surface plasmon resonance assay for the binding of influenza virus hemagglutinin to its sialic acid receptor.* Virology, 1996. **217**(2): p. 452-8.
95. Huotari, J. and A. Helenius, *Endosome maturation.* EMBO J, 2011. **30**(17): p. 3481-500.
96. Bullough, P.A., et al., *Structure of influenza haemagglutinin at the pH of membrane fusion.* Nature, 1994. **371**(6492): p. 37-43.

97. Durrer, P., et al., *H+-induced membrane insertion of influenza virus hemagglutinin involves the HA2 amino-terminal fusion peptide but not the coiled coil region.* J Biol Chem, 1996. **271**(23): p. 13417-21.
98. Skehel, J.J., et al., *Changes in the conformation of influenza virus hemagglutinin at the pH optimum of virus-mediated membrane fusion.* Proc Natl Acad Sci U S A, 1982. **79**(4): p. 968-72.
99. Spruce, A.E., et al., *Patch clamp studies of single cell-fusion events mediated by a viral fusion protein.* Nature, 1989. **342**(6249): p. 555-8.
100. Harrison, S.C., *Viral membrane fusion.* Nat Struct Mol Biol, 2008. **15**(7): p. 690-8.
101. Skehel, J.J. and D.C. Wiley, *Receptor binding and membrane fusion in virus entry: the influenza hemagglutinin.* Annu Rev Biochem, 2000. **69**: p. 531-69.
102. Yoshimura, A., et al., *Infectious cell entry mechanism of influenza virus.* J Virol, 1982. **43**(1): p. 284-93.
103. Braakman, I., et al., *Folding of influenza hemagglutinin in the endoplasmic reticulum.* J Cell Biol, 1991. **114**(3): p. 401-11.
104. Scheiffele, P., et al., *Influenza viruses select ordered lipid domains during budding from the plasma membrane.* J Biol Chem, 1999. **274**(4): p. 2038-44.
105. Barman, S., et al., *Transport of viral proteins to the apical membranes and interaction of matrix protein with glycoproteins in the assembly of influenza viruses.* Virus Res, 2001. **77**(1): p. 61-9.
106. Scheiffele, P., M.G. Roth, and K. Simons, *Interaction of influenza virus haemagglutinin with sphingolipid-cholesterol membrane domains via its transmembrane domain.* EMBO J, 1997. **16**(18): p. 5501-8.
107. Zhang, J., A. Pekosz, and R.A. Lamb, *Influenza virus assembly and lipid raft microdomains: a role for the cytoplasmic tails of the spike glycoproteins.* J Virol, 2000. **74**(10): p. 4634-44.
108. Schmitt, A.P. and R.A. Lamb, *Influenza virus assembly and budding at the viral budozone.* Adv Virus Res, 2005. **64**: p. 383-416.
109. Zhang, J., et al., *The cytoplasmic tails of the influenza virus spike glycoproteins are required for normal genome packaging.* Virology, 2000. **269**(2): p. 325-34.
110. Pattnaik, A.K., D.J. Brown, and D.P. Nayak, *Formation of influenza virus particles lacking hemagglutinin on the viral envelope.* J Virol, 1986. **60**(3): p. 994-1001.
111. McGrath, M.E., *The lysosomal cysteine proteases.* Annu Rev Biophys Biomol Struct, 1999. **28**: p. 181-204.
112. Ha, S.D., et al., *Cathepsin B is involved in the trafficking of TNF-alpha-containing vesicles to the plasma membrane in macrophages.* J Immunol, 2008. **181**(1): p. 690-7.
113. Duncan, J.A., et al., *Neisseria gonorrhoeae activates the proteinase cathepsin B to mediate the signaling activities of the NLRP3 and ASC-containing inflammasome.* J Immunol, 2009. **182**(10): p. 6460-9.
114. Hornung, V., et al., *Silica crystals and aluminum salts activate the NALP3 inflammasome through phagosomal destabilization.* Nat Immunol, 2008. **9**(8): p. 847-56.
115. Willingham, S.B., et al., *Microbial pathogen-induced necrotic cell death mediated by the inflammasome components CIAS1/cryopyrin/NLRP3 and ASC.* Cell Host Microbe, 2007. **2**(3): p. 147-59.

116. Esser, R.E., et al., *Cysteine proteinase inhibitors decrease articular cartilage and bone destruction in chronic inflammatory arthritis.* Arthritis Rheum, 1994. **37**(2): p. 236-47.
117. Yan, S., M. Sameni, and B.F. Sloane, *Cathepsin B and human tumor progression.* Biol Chem, 1998. **379**(2): p. 113-23.
118. Pucer, A., et al., *Differential role of cathepsins B and L in autophagy-associated cell death induced by arsenic trioxide in U87 human glioblastoma cells.* Biol Chem, 2010. **391**(5): p. 519-31.
119. Bruchard, M., et al., *Chemotherapy-triggered cathepsin B release in myeloid-derived suppressor cells activates the Nlrp3 inflammasome and promotes tumor growth.* Nat Med, 2013. **19**(1): p. 57-64.
120. Reiser, J., B. Adair, and T. Reinheckel, *Specialized roles for cysteine cathepsins in health and disease.* J Clin Invest, 2010. **120**(10): p. 3421-31.
121. Mason, R.W., *Lysosomal Metabolism of Proteins*, in *Biology of the Lysosome*, J.B. Lloyd, Mason, R.W. , Editor. 1996, Plenum Press: New York. p. 159-190.
122. Turk, B., D. Turk, and V. Turk, *Lysosomal cysteine proteases: more than scavengers.* BBActa-Protein Struct M, 2000. **1477**(1-2): p. 98-111.
123. Stachowiak, K., et al., *Fluorogenic peptide substrates for carboxydipeptidase activity of cathepsin B.* Acta Biochim Pol, 2004. **51**(1): p. 81-92.
124. Guicciardi, M.E., et al., *Cathepsin B contributes to TNF-alpha-mediated hepatocyte apoptosis by promoting mitochondrial release of cytochrome c.* J Clin Invest, 2000. **106**(9): p. 1127-37.
125. Roshy, S., B.F. Sloane, and K. Moin, *Pericellular cathepsin B and malignant progression.* Cancer Metastasis Rev, 2003. **22**(2-3): p. 271-86.
126. Riccio, M., et al., *Nuclear localization of cystatin B, the cathepsin inhibitor implicated in myoclonus epilepsy (EPM1).* Exp Cell Res, 2001. **262**(2): p. 84-94.
127. Blum, J.S., M.L. Fiani, and P.D. Stahl, *Proteolytic cleavage of ricin A chain in endosomal vesicles. Evidence for the action of endosomal proteases at both neutral and acidic pH.* J Biol Chem, 1991. **266**(33): p. 22091-5.
128. Creemers, L.B., et al., *Participation of intracellular cysteine proteinases, in particular cathepsin B, in degradation of collagen in periosteal tissue explants.* Matrix Biol, 1998. **16**(9): p. 575-84.
129. Lindkvist, B., et al., *Cathepsin B activates human trypsinogen 1 but not proelastase 2 or procarboxypeptidase B.* Pancreatology, 2006. **6**(3): p. 224-31.
130. Blomgran, R., L. Zheng, and O. Stendahl, *Cathepsin-cleaved Bid promotes apoptosis in human neutrophils via oxidative stress-induced lysosomal membrane permeabilization.* J Leukoc Biol, 2007. **81**(5): p. 1213-23.
131. Michallet, M.C., et al., *Cathepsin-B-dependent apoptosis triggered by antithymocyte globulins: a novel mechanism of T-cell depletion.* Blood, 2003. **102**(10): p. 3719-26.
132. Zhao, X.S., et al., *Effect of cathepsin B on thymocyte apoptosis in spontaneously hypertensive rats.* Acta Pharmacol Sin, 2001. **22**(1): p. 26-31.
133. Foghsgaard, L., et al., *Cathepsin B acts as a dominant execution protease in tumor cell apoptosis induced by tumor necrosis factor.* J Cell Biol, 2001. **153**(5): p. 999-1010.
134. Turk, B., D. Turk, and G.S. Salvesen, *Regulating cysteine protease activity: Essential role of protease inhibitors as guardians and regulators.* Curr Pharm Design, 2002. **8**(18): p. 1623-1637.

135. Turk, B., V. Turk, and D. Turk, *Structural and functional aspects of papain-like cysteine proteinases and their protein inhibitors.* Biol Chem, 1997. **378**(3-4): p. 141-50.
136. Ebert, D.H., et al., *Cathepsin L and cathepsin B mediate reovirus disassembly in murine fibroblast cells.* J Biol Chem, 2002. **277**(27): p. 24609-17.
137. Ha, S.D., et al., *Inhibition or deficiency of cathepsin B leads defects in HIV-1 Gag pseudoparticle release in macrophages and HEK293T cells.* Antiviral Res, 2011.
138. Kumar, P., et al., *Host cell Cathepsins potentiate Moloney murine leukemia virus infection.* J Virol, 2007. **81**(19): p. 10506-10514.
139. Yoshii, H., et al., *CD4-independent human immunodeficiency virus infection involves participation of endocytosis and cathepsin B.* PLoS One, 2011. **6**(4): p. e19352.
140. Steverding, D., *The Cathepsin B-Selective Inhibitors CA-074 and CA-074Me Inactivate Cathepsin L Under Reducing Conditions.* Open Enzym Inhib J, 2011. **4**: p. 11-16.
141. Sloane, B.F., J.R. Dunn, and K.V. Honn, *Lysosomal cathepsin B: correlation with metastatic potential.* Science, 1981. **212**(4499): p. 1151-3.
142. Hirano, T. and S. Takeuchi, *Serum cathepsin-B levels and urinary-excretion of cathepsin-B in the patients with colorectal-cancer - possible indicators for tumor malignancy.* Int J Oncol, 1994. **4**(1): p. 151-3.
143. Fernandez, P.L., et al., *Expression of cathepsins B and S in the progression of prostate carcinoma.* Int J Cancer, 2001. **95**(1): p. 51-5.
144. Victor, B.C., et al., *Inhibition of cathepsin B activity attenuates extracellular matrix degradation and inflammatory breast cancer invasion.* Breast Cancer Res, 2011. **13**(6).
145. Chu, S.C., et al., *Cathepsin B and cystatin C play an inflammatory role in gouty arthritis of the knee.* Clin Chim Acta, 2010. **411**(21-22): p. 1788-92.
146. Mishiro, T., et al., *Relationship between cathepsin B and thrombin in rheumatoid arthritis.* J Rheumatol, 2004. **31**(7): p. 1265-73.
147. Hashimoto, Y., et al., *Significance of cathepsin B accumulation in synovial fluid of rheumatoid arthritis.* Biochem Biophys Res Commun, 2001. **283**(2): p. 334-9.
148. Hansen, T., et al., *Cathepsin B and its endogenous inhibitor cystatin C in rheumatoid arthritis synovium.* J Rheumatol, 2000. **27**(4): p. 859-65.
149. Mueller-Steiner, S., et al., *Antiamyloidogenic and neuroprotective functions of cathepsin B: implications for Alzheimer's disease.* Neuron, 2006. **51**(6): p. 703-14.
150. Tertov, V.V. and A.N. Orekhov, *Metabolism of native and naturally occurring multiple modified low density lipoprotein in smooth muscle cells of human aortic intima.* Exp Mol Pathol, 1997. **64**(3): p. 127-45.
151. Chandran, K., et al., *Endosomal proteolysis of the Ebola virus glycoprotein is necessary for infection.* Science, 2005. **308**(5728): p. 1643-5.
152. Nanbo, A., et al., *Ebolavirus is internalized into host cells via macropinocytosis in a viral glycoprotein-dependent manner.* PLoS Pathog, 2010. **6**(9): p. e1001121.
153. Gnirss, K., et al., *Cathepsins B and L activate Ebola but not Marburg virus glycoproteins for efficient entry into cell lines and macrophages independent of TMPRSS2 expression.* Virology, 2012. **424**(1): p. 3-10.
154. Schornberg, K., et al., *Role of endosomal cathepsins in entry mediated by the Ebola virus glycoprotein.* J Virol, 2006. **80**(8): p. 4174-8.

155. Marzi, A., T. Reinheckel, and H. Feldmann, *Cathepsin B & L are not required for ebola virus replication.* PLoS Negl Trop Dis, 2012. **6**(12): p. e1923.
156. Diederich, S., et al., *Activation of the Nipah Virus Fusion Protein in MDCK Cells Is Mediated by Cathepsin B within the Endosome-Recycling Compartment.* J Virol, 2012. **86**(7): p. 3736-3745.
157. Regan, A.D., et al., *Differential role for low pH and cathepsin-mediated cleavage of the viral spike protein during entry of serotype II feline coronaviruses.* Vet Microbiol, 2008. **132**(3-4): p. 235-248.
158. Akache, B., et al., *A two-hybrid screen identifies cathepsins B and L as uncoating factors for adeno-associated virus 2 and 8.* Mol Ther, 2007. **15**(2): p. 330-9.
159. Link, M.A., L.A. Silva, and P.A. Schaffer, *Cathepsin B mediates cleavage of herpes simplex virus type 1 origin binding protein (OBP) to yield OBPC-1, and cleavage is dependent upon viral DNA replication.* J Virol, 2007. **81**(17): p. 9175-82.
160. Cantres-Rosario, Y., et al., *Cathepsin B and cystatin B in HIV-seropositive women are associated with infection and HIV-1-associated neurocognitive disorders.* AIDS, 2013. **27**(3): p. 347-356.
161. Qin, Y.W. and G.P. Shi, *Cysteinyl cathepsins and mast cell proteases in the pathogenesis and therapeutics of cardiovascular diseases.* Pharmacol Therapeut, 2011. **131**(3): p. 338-350.
162. Lutgens, S.P.M., et al., *Cathepsin cysteine proteases in cardiovascular disease.* Faseb Journal, 2007. **21**(12): p. 3029-3041.
163. Tertov, V.V. and A.N. Orekhov, *Metabolism of native and naturally occurring multiple modified low density lipoprotein in smooth muscle cells of human aortic intima.* Exp Mol Pathol, 1997. **64**(3): p. 127-145.
164. Haidar, B., et al., *Cathepsin D, a lysosomal protease, regulates ABCA1-mediated lipid efflux.* J Biol Chem, 2006. **281**(52): p. 39971-81.
165. Liao, G., et al., *Cholesterol accumulation is associated with lysosomal dysfunction and autophagic stress in Npc1 -/- mouse brain.* Am J Pathol, 2007. **171**(3): p. 962-75.
166. Carstea, E.D., et al., *Niemann-Pick C1 disease gene: homology to mediators of cholesterol homeostasis.* Science, 1997. **277**(5323): p. 228-31.
167. Ko, D.C., et al., *Dynamic movements of organelles containing Niemann-Pick C1 protein: NPC1 involvement in late endocytic events.* Mol Biol Cell, 2001. **12**(3): p. 601-14.
168. Liscum, L., *Niemann-Pick type C mutations cause lipid traffic jam.* Traffic, 2000. **1**(3): p. 218-25.
169. te Vruchte, D., et al., *Accumulation of glycosphingolipids in Niemann-Pick C disease disrupts endosomal transport.* J Biol Chem, 2004. **279**(25): p. 26167-75.
170. Adami, C., M.J. Brunda, and A.V. Palleroni, *In vivo immortalization of murine peritoneal macrophages: a new rapid and efficient method for obtaining macrophage cell lines.* J Leukoc Biol, 1993. **53**(4): p. 475-8.
171. Shelton, H., et al., *An influenza reassortant with polymerase of pH1N1 and NS gene of H3N2 influenza A virus is attenuated in vivo.* J Gen Virol, 2012. **93**(Pt 5): p. 998-1006.
172. Ngaosuwankul, N., et al., *Influenza A viral loads in respiratory samples collected from patients infected with pandemic H1N1, seasonal H1N1 and H3N2 viruses.* Virol J, 2010. **7**: p. 75.

173. Fouchier, R.A., et al., *Detection of influenza A viruses from different species by PCR amplification of conserved sequences in the matrix gene.* J Clin Microbiol, 2000. **38**(11): p. 4096-101.
174. Folch, J., M. Lees, and G.H. Sloane Stanley, *A simple method for the isolation and purification of total lipides from animal tissues.* J Biol Chem, 1957. **226**(1): p. 497-509.
175. Folch, J., et al., *Preparation of lipide extracts from brain tissue.* J Biol Chem, 1951. **191**(2): p. 833-41.
176. Bradford, M.M., *A rapid and sensitive method for the quantitation of microgram quantities of protein utilizing the principle of protein-dye binding.* Anal Biochem, 1976. **72**: p. 248-54.
177. Bolte, S. and F.P. Cordelieres, *A guided tour into subcellular colocalization analysis in light microscopy.* J Microsc-Oxford, 2006. **224**: p. 213-232.
178. Killian, M.L., *Hemagglutination assay for the avian influenza virus.* Methods Mol Biol, 2008. **436**: p. 47-52.
179. Chou, Y.Y., et al., *One influenza virus particle packages eight unique viral RNAs as shown by FISH analysis.* Proc Natl Acad Sci U S A, 2012. **109**(23): p. 9101-6.
180. Liu, S.L., et al., *Effectively and Efficiently Dissecting the Infection of Influenza Virus by Quantum-Dot-Based Single-Particle Tracking.* ACS Nano, 2012. **6**(1): p. 141-150.
181. Thaa, B., et al., *Growth of influenza A virus is not impeded by simultaneous removal of the cholesterol-binding and acylation sites in the M2 protein.* J Gen Virol, 2012. **93**(Pt 2): p. 282-92.
182. Zhou, Z., et al., *Lysosome-associated membrane glycoprotein 3 is involved in influenza A virus replication in human lung epithelial (A549) cells.* Virol J, 2011. **8**: p. 384.
183. Gannage, M., et al., *Matrix protein 2 of influenza A virus blocks autophagosome fusion with lysosomes.* Cell Host Microbe, 2009. **6**(4): p. 367-80.
184. Feeley, E.M., et al., *IFITM3 Inhibits Influenza A Virus Infection by Preventing Cytosolic Entry.* Plos Pathogens, 2011. **7**(10).
185. Shaw, M.L., et al., *Cellular proteins in influenza virus particles.* PLoS Pathog, 2008. **4**(6): p. e1000085.
186. Beaulieu, A., et al., *Matriptase proteolytically activates influenza virus and promotes multicycle replication in the human airway epithelium.* J Virol, 2013. **87**(8): p. 4237-51.
187. Ha, S.D., et al., *Cathepsin B-mediated autophagy flux facilitates the anthrax toxin receptor 2-mediated delivery of anthrax lethal factor into the cytoplasm.* J Biol Chem, 2010. **285**(3): p. 2120-9.
188. Hebert, D.N. and M. Molinari, *In and out of the ER: Protein folding, quality control, degradation, and related human diseases.* Physiol Rev, 2007. **87**(4): p. 1377-1408.
189. Della Valle, M.C., et al., *Classification of subcellular location by comparative proteomic analysis of native and density-shifted lysosomes.* Mol Cell Proteomics, 2011. **10**(4): p. M110 006403.
190. Filocamo, M. and A. Morrone, *Lysosomal storage disorders: molecular basis and laboratory testing.* Hum Genomics, 2011. **5**(3): p. 156-69.
191. Sun, X. and G.R. Whittaker, *Role for influenza virus envelope cholesterol in virus entry and infection.* J Virol, 2003. **77**(23): p. 12543-51.

192. Leser, G.P. and R.A. Lamb, *Influenza virus assembly and budding in raft-derived microdomains: A quantitative analysis of the surface distribution of HA, NA and M2 proteins.* Virology, 2005. **342**(2): p. 215-227.
193. Barman, S. and D.P. Nayak, *Lipid raft disruption by cholesterol depletion enhances influenza A virus budding from MDCK cells.* J Virol, 2007. **81**(22): p. 12169-78.
194. Stewart, S.M., et al., *The cholesterol recognition/interaction amino acid consensus motif of the influenza A virus M2 protein is not required for virus replication but contributes to virulence.* Virology, 2010. **405**(2): p. 530-8.
195. Keller, P. and K. Simons, *Cholesterol is required for surface transport of influenza virus hemagglutinin.* J Cell Biol, 1998. **140**(6): p. 1357-1367.
196. Carrasco, M., M.J. Amorim, and P. Digard, *Lipid raft-dependent targeting of the influenza A virus nucleoprotein to the apical plasma membrane.* Traffic, 2004. **5**(12): p. 979-92.
197. Hatada, E., et al., *Control of influenza virus gene expression: quantitative analysis of each viral RNA species in infected cells.* J Biochem, 1989. **105**(4): p. 537-46.
198. Vogel, U. and C. Scholtissek, *Inhibition of the intracellular transport of influenza viral RNA by actinomycin D.* Arch Virol, 1995. **140**(10): p. 1715-23.
199. Skehel, J.J. and A.J. Hay, *Influenza virus transcription.* J Gen Virol, 1978. **39**(1): p. 1-8.
200. Petri, T., H. Meierewert, and R.W. Compans, *Inhibition of Influenza-C Virus-Replication by Actinomycin-D, Alpha Amanitin, and Uv Irradiation.* J Virol, 1979. **32**(3): p. 1037-1040.
201. Vogel, U. and C. Scholtissek, *Inhibition of the Intracellular-Transport of Influenza Viral-Rna by Actinomycin-D.* Arch Virol, 1995. **140**(10): p. 1715-1723.
202. Vreede, F.T., et al., *Stabilization of Influenza Virus Replication Intermediates Is Dependent on the RNA-Binding but Not the Homo-Oligomerization Activity of the Viral Nucleoprotein (vol 85, pg 12073, 2011).* J Virol, 2012. **86**(1): p. 640-640.
203. Dovas, C.I., et al., *Detection and quantification of infectious avian influenza A (H5N1) virus in environmental water by using real-time reverse transcription-PCR.* Appl Environ Microbiol, 2010. **76**(7): p. 2165-74.
204. Vester, D., et al., *Real-time RT-qPCR assay for the analysis of human influenza A virus transcription and replication dynamics.* J Virol Methods, 2010. **168**(1-2): p. 63-71.
205. Yoshikawa, T., et al., *Total viral genome copies and virus-Ig complexes after infection with influenza virus in the nasal secretions of immunized mice.* J Gen Virol, 2004. **85**(Pt 8): p. 2339-46.
206. D. P. Nayak, N.S., *The Structure of Influenza Virus Defective Interfering (DI) RNAs and Their Progenitor Genes*, in *Genetics of Influenza Viruses*, D.W.K. Peter Palese, Editor. 1983. p. 255-279
207. Nayak, D.P., *Defective interfering influenza viruses.* Annu Rev Microbiol, 1980. **34**: p. 619-44.
208. Von Magnus, P., *Propagation of the PR8 strain of influenza A virus in chick embryos. III. Properties of the incomplete virus produced in serial passages of undiluted virus.* Acta Pathol Microbiol Scand, 1951. **29**(2): p. 157-81.
209. Carpenter, J.E., E.P. Henderson, and C. Grose, *Enumeration of an extremely high particle-to-PFU ratio for Varicella-zoster virus.* J Virol, 2009. **83**(13): p. 6917-21.

210. Marriott, A.C. and N.J. Dimmock, *Defective interfering viruses and their potential as antiviral agents.* Rev Med Virol, 2010. **20**(1): p. 51-62.
211. Yu, W.C., et al., *Viral replication and innate host responses in primary human alveolar epithelial cells and alveolar macrophages infected with influenza H5N1 and H1N1 viruses.* J Virol, 2011. **85**(14): p. 6844-55.
212. Gomez-Puertas, P., et al., *Influenza virus matrix protein is the major driving force in virus budding.* J Virol, 2000. **74**(24): p. 11538-11547.
213. Meier-Ewert, H. and R.W. Compans, *Time course of synthesis and assembly of influenza virus proteins.* J Virol, 1974. **14**(5): p. 1083-91.
214. Landeras-Bueno, S., et al., *The Splicing Factor Proline-Glutamine Rich (SFPQ/PSF) Is Involved in Influenza Virus Transcription.* Plos Pathogens, 2011. **7**(11).
215. Yang, C., et al., *Deliberate reduction of hemagglutinin and neuraminidase expression of influenza virus leads to an ultraprotective live vaccine in mice.* Proc Natl Acad Sci U S A, 2013. **110**(23): p. 9481-6.
216. Emma, P. and A. Kamen, *Real-time monitoring of influenza virus production kinetics in HEK293 cell cultures.* Biotechnol Prog, 2013. **29**(1): p. 275-84.
217. Stow, J.L., et al., *Cytokine secretion in macrophages and other cells: pathways and mediators.* Immunobiology, 2009. **214**(7): p. 601-12.
218. Cooper, G.M., *Protein Degradation*, in *The Cell: A Molecular Approach*. 2000, Sinauer Associates.
219. Jaillais, Y., et al., *Evidence for a sorting endosome in Arabidopsis root cells.* Plant J, 2008. **53**(2): p. 237-247.
220. Fujita, H., et al., *Inulavosin, a Melanogenesis Inhibitor, Leads to Mistargeting of Tyrosinase to Lysosomes and Accelerates its Degradation.* J Invest Dermatol, 2009. **129**(6): p. 1489-1499.
221. Fujita, H., et al., *Evidence for distinct membrane traffic pathways to melanosomes and lysosomes in melanocytes.* J Invest Derm Symp P, 2001. **6**(1): p. 19-24.
222. Probes, M. *LysoTracker® and LysoSensor™ Probes*. 2007 June 20/13]; Available from: http://probes.invitrogen.com/media/pis/mp07525.pdf.
223. Zinchuk, V. and O. Zinchuk, *Quantitative colocalization analysis of confocal fluorescence microscopy images.* Curr Protoc Cell Biol, 2008. **Chapter 4**: p. Unit 4 19.
224. Freundt, E.C., M. Czapiga, and M.J. Lenardo, *Photoconversion of Lysotracker Red to a green fluorescent molecule.* Cell Res, 2007. **17**(11): p. 956-958.
225. Tang, Y., et al., *Deficiency of niemann-pick type C-1 protein impairs release of human immunodeficiency virus type 1 and results in Gag accumulation in late endosomal/lysosomal compartments.* J Virol, 2009. **83**(16): p. 7982-95.
226. Coleman, E.M., T.N. Walker, and J.E. Hildreth, *Loss of Niemann Pick type C proteins 1 and 2 greatly enhances HIV infectivity and is associated with accumulation of HIV Gag and cholesterol in late endosomes/lysosomes.* Virol J, 2012. **9**: p. 31.
227. Cote, M., et al., *Small molecule inhibitors reveal Niemann-Pick C1 is essential for Ebola virus infection.* Nature, 2011. **477**(7364): p. 344-8.
228. Carette, J.E., et al., *Ebola virus entry requires the cholesterol transporter Niemann-Pick C1.* Nature, 2011. **477**(7364): p. 340-3.
229. Isaacsohn, J., *Chapter 4: The Role of Cholesterol*. Yale University School of Medicine Heart Book, ed. M.M. Barry L. Zaret, Lawrence S. Cohen. 1992: Yale University.

230. Wang, X., E.R. Hinson, and P. Cresswell, *The interferon-inducible protein viperin inhibits influenza virus release by perturbing lipid rafts.* Cell Host Microbe, 2007. **2**(2): p. 96-105.
231. Vandermeer, M.L., et al., *Association between use of statins and mortality among patients hospitalized with laboratory-confirmed influenza virus infections: a multistate study.* J Infect Dis, 2012. **205**(1): p. 13-9.
232. Fedson, D.S., *Pandemic influenza: a potential role for statins in treatment and prophylaxis.* Clin Infect Dis, 2006. **43**(2): p. 199-205.
233. Burster, T., et al., *Influenza A virus elevates active cathepsin B in primary murine DC.* Int Immunol, 2007. **19**(5): p. 645-655.
234. Chapman, H.A., *Cathepsins as transcriptional activators?* Dev Cell, 2004. **6**(5): p. 610-1.
235. Maubach, G., M.C. Lim, and L. Zhuo, *Nuclear cathepsin F regulates activation markers in rat hepatic stellate cells.* Mol Biol Cell, 2008. **19**(10): p. 4238-48.
236. Comber, J.D., et al., *Functional Macroautophagy Induction by Influenza A Virus without a Contribution to Major Histocompatibility Complex Class II-Restricted Presentation.* J Virol, 2011. **85**(13): p. 6453-6463.
237. Zhou, Z., et al., *Autophagy is involved in influenza A virus replication.* Autophagy, 2009. **5**(3): p. 321-328.
238. Ma, J.H., et al., *Avian influenza A virus H5N1 causes autophagy-mediated cell death through suppression of mTOR signaling.* J Genet Genomics, 2011. **38**(11): p. 533-537.
239. Rossman, J.S. and R.A. Lamb, *Autophagy, apoptosis, and the influenza virus M2 protein.* Cell Host Microbe, 2009. **6**(4): p. 299-300.
240. McLean, J.E., et al., *Lack of Bax prevents influenza A virus-induced apoptosis and causes diminished viral replication.* J Virol, 2009. **83**(16): p. 8233-46.
241. Zhirnov, O.P. and H.D. Klenk, *Control of apoptosis in influenza virus-infected cells by up-regulation of Akt and p53 signaling.* Apoptosis, 2007. **12**(8): p. 1419-32.
242. Shiozaki, T., et al., *Requirement for Siva-1 for replication of influenza A virus through apoptosis induction.* J Gen Virol, 2011. **92**(Pt 2): p. 315-25.
243. Uchiyama, Y., *Autophagic cell death and its execution by lysosomal cathepsins.* Arch Histol Cytol, 2001. **64**(3): p. 233-46.
244. Bhoopathi, P., et al., *Cathepsin B facilitates autophagy-mediated apoptosis in SPARC overexpressed primitive neuroectodermal tumor cells.* Cell Death Differ, 2010. **17**(10): p. 1529-39.
245. Lamore, S.D. and G.T. Wondrak, *Autophagic-lysosomal dysregulation downstream of cathepsin B inactivation in human skin fibroblasts exposed to UVA.* Photochem Photobiol Sci, 2011.
246. Ichinohe, T., I.K. Pang, and A. Iwasaki, *Influenza virus activates inflammasomes via its intracellular M2 ion channel.* Nat Immunol, 2010. **11**(5): p. 404-10.
247. Wurzer, W.J., et al., *Caspase 3 activation is essential for efficient influenza virus propagation.* EMBO J, 2003. **22**(11): p. 2717-28.
248. Herold, S., et al., *Apoptosis signaling in influenza virus propagation, innate host defense, and lung injury.* J Leukoc Biol, 2012. **92**(1): p. 75-82.
249. Malla, R.R., et al., *uPAR and cathepsin B downregulation induces apoptosis by targeting calcineurin A to BAD via Bcl-2 in glioma.* J Neurooncol, 2012. **107**(1): p. 69-80.

250. Garcia-Cattaneo, A., et al., *Cleavage of Toll-like receptor 3 by cathepsins B and H is essential for signaling.* Proc Natl Acad Sci U S A, 2012. **109**(23): p. 9053-8.
251. Deyde, V.M., et al., *Surveillance of resistance to adamantanes among influenza A(H3N2) and A(H1N1) viruses isolated worldwide.* J Infect Dis, 2007. **196**(2): p. 249-57.
252. Fiore, A.E., et al., *Antiviral agents for the treatment and chemoprophylaxis of influenza --- recommendations of the Advisory Committee on Immunization Practices (ACIP).* MMWR Recomm Rep, 2011. **60**(1): p. 1-24.
253. Monto, A.S., *Implications of antiviral resistance of influenza viruses.* Clin Infect Dis, 2009. **48**(4): p. 397-9.
254. Hayden, F.G. and M.D. de Jong, *Emerging influenza antiviral resistance threats.* J Infect Dis, 2011. **203**(1): p. 6-10.
255. Ananthanarayan, R. and C.K. Paniker, *Non-specific inhibitors of influenza viruses in normal sera.* Bull World Health Organ, 1960. **22**: p. 409-19.
256. Hartley, C.A., D.C. Jackson, and E.M. Anders, *Two distinct serum mannose-binding lectins function as beta inhibitors of influenza virus: identification of bovine serum beta inhibitor as conglutinin.* J Virol, 1992. **66**(7): p. 4358-63.
257. Choppin, P.W. and I. Tamm, *Studies of two kinds of virus particles which comprise influenza A2 virus strains. II. Reactivity with virus inhibitors in normal sera.* J Exp Med, 1960. **112**: p. 921-44.
258. Anders, E.M., C.A. Hartley, and D.C. Jackson, *Bovine and mouse serum beta inhibitors of influenza A viruses are mannose-binding lectins.* Proc Natl Acad Sci U S A, 1990. **87**(12): p. 4485-9.

Chapter 6: Appendices

Appendix 1 – ActD blocks the production of viral HA protein at a concentration of 5 µg/mL.

A549 cells were infected with influenza at an MOI of 1 in the presence or absence of ActD (5 µg/mL) for six hours. After infection, the cells were harvested, lysed, and subjected to Western blotting for HA as described in "Methods". There were no immunoreactivities for HA detected in either condition receiving ActD, indicating the viral protein was not produced in detectable quantities.

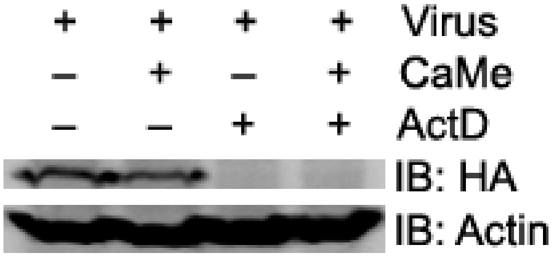
+ + + + Virus
– + – + CaMe
– – + + ActD
IB: HA
IB: Actin

Appendix 2 – Detected copy numbers of HA and MA per titred virion in the inoculum.

1.0×10^4 virions from the inoculum used in this study were subjected to RNA extraction as described in "Methods". One µL of the resulting RNA was used for each reverse transcription reaction. cDNA was then used for qPCR amplification following the same conditions used for experimental procedures. Ct values obtained were converted to copy numbers using the standard curve equations in Figure 3, and dilution factors were used to calculate the gene copies/titred virion from the original inoculum (n=3). Data are expressed as means ± SEM.

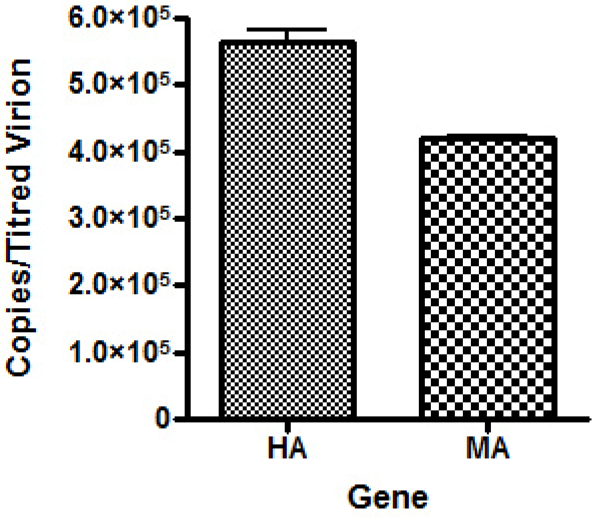
Copies/Titred Virion
6.0×10⁵
5.0×10⁵
4.0×10⁵
3.0×10⁵
2.0×10⁵
1.0×10⁵
0
HA
MA
Gene

Appendix 3 – Immunofluorescence microscopy of infected A549 cells stained with 2□ antibody (FITC) only.

Coverslips with adherent A549 cells were infected for six hours at a high MOI (>10). 5.5 hours post-infection, LysoTracker Red was added to a final concentration of 200 nM and allowed to incubate for 30 min. At 6 hours, coverslips were removed from virus-containing medium, fixed in 4% formaldehyde, and blocked in PBS + 1% BSA + 0.05% Tween 20 for 1 hour. Coverslips were then washed in PBS and incubated in secondary antibody (anti-mouse FITC) at a 1:100 dilution for 2 hours. Slides were washed once more and incubated in Hoechst 33342 for 3 min at a 1:4000 dilution, rinsed, mounted, and viewed using a Bio-Rad Radiance 2000 fluorescence microscope.

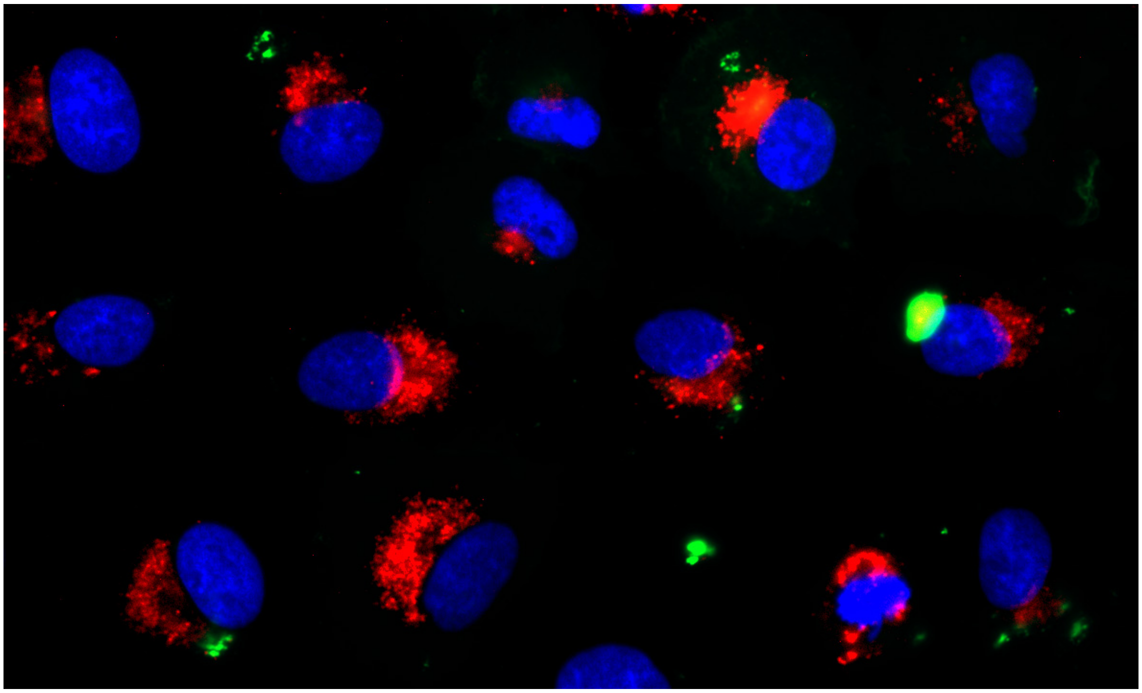

Appendix 4 – Hemagglutination assay of infected A549 supernatants

1.0 x10^6 A549 cells were infected at an MOI of 1 as described in “Methods” in the presence or absence of different concentrations of CaMe in the absence of serum, which contains nonspecific inhibitors of IVA infection [255-258]. After 24 hours, supernatants were removed from monolayers and subjected to a standard hemagglutination assay using chicken red blood cells and a series of two-fold dilutions of the supernatants. After a 30 min incubation, wells were scored as being either positive or negative for agglutination, and the titer expressed as the reciprocal of the highest dilution yielding agglutination. (**A**) A representative image of hemagglutination assay results, with both negative (–) and positive (+) controls. (**B**) There was no significant difference between the titre of untreated cells and cells treated with 150 µM CaMe, but 500 µM CaMe treatment showed a significant reduction in virus titre ($p > 0.05$; one-way ANOVA; $n \geq 3$). Data are expressed as means ± SEM from at least three independent experiments. Columns accompanied by the same letter are not significantly different from each other by Tukey’s post hoc test.

A

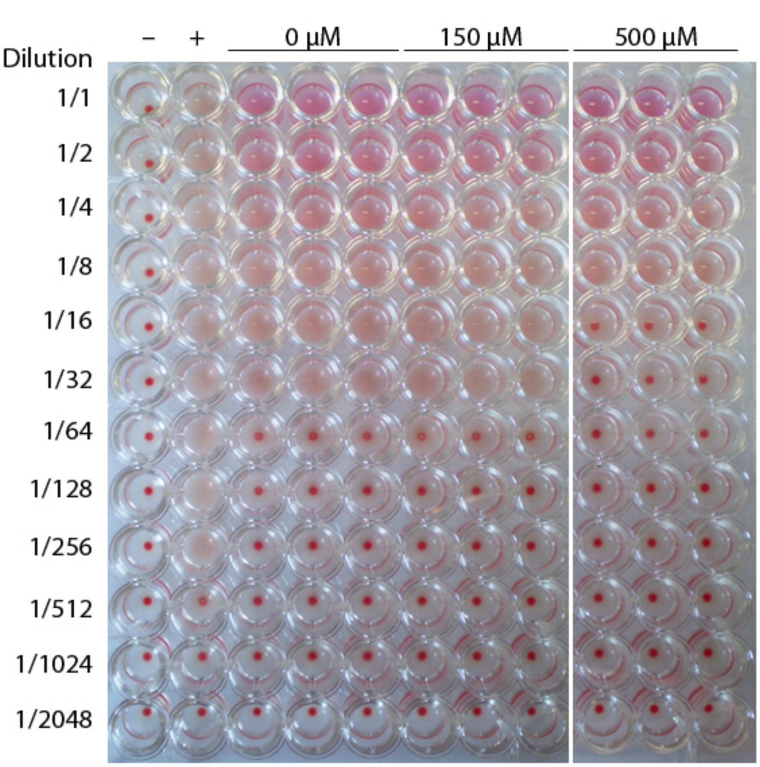
−
+
0 μM
150 μM
500 μM
Dilution
1/1
1/2
1/4
1/8
1/16
1/32
1/64
1/128
1/256
1/512
1/1024
1/2048

B

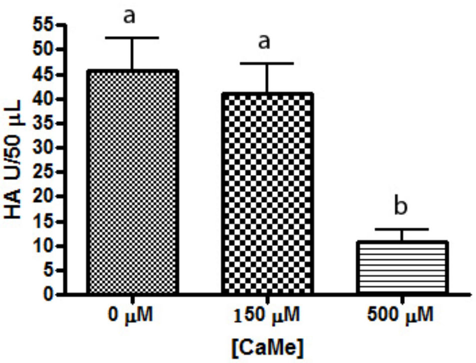
a
a
b
55
50
45
40
35
30
25
20
15
10
5
0
HA U/50 μL
0 μM
150 μM
500 μM
[CaMe]

Chapter 7: Curriculum Vitae

Macon Coleman

Education

MSc Candidate 2011-2013
Department of Microbiology & Immunology
Western University, London ON

BMSc, Honors Specialization Microbiology & Immunology 2007-2011
The University of Western Ontario, London ON
Dean's Honor List

Publications

Sangwook Park, Soon-Duck Ha, **Macon Coleman**, Shahab Meshkibaf, Sung Ouk Kim, *p62/SQSTM1 enhances NOD2-mediated signaling and cytokine production through stabilizing NOD2 oligomerization.* PLoS One, 2013. **8**(2): p. e57138. doi:10.1371/journal.pone.0057138

Matthew W. Woods, Jenna N. Kelly, Clayton J. Hattlmann, Jessica G.K. Tong, Li S. Xu, **Macon D. Coleman**, Graeme R. Quest, James, R. Smiley, Stephen D. Barr. *Human HERC5 restricts an early stage of HIV-1 assembly by a mechanism correlating with the ISGylation of Gag.* Retrovirology, 2011. **8**:95.

Scholarships & Awards

Schulich Graduate Scholarship	2011
Western Scholarship of Distinction	2007

Teaching Experience

Teaching Assistant: 2500B The Biology of Infection and Immunity 2013
Western University, Department of Microbiology and Immunology

- Arranged and held review sessions, assisted with content-based questions
- Proctored examinations

Forth Year Honors Student 2011-2012
Western University, Department of Microbiology and Immunology

- Assisted in the planning and execution of experiments
- Aided in the written and oral communication of experimental findings